ORNL-3551
UC-25 – Metals, Ceramics, and Materials
TID-4500 (26th ed.)

CORROSION OF REFRACTORY METALS BY LITHIUM

James Richard DiStefano

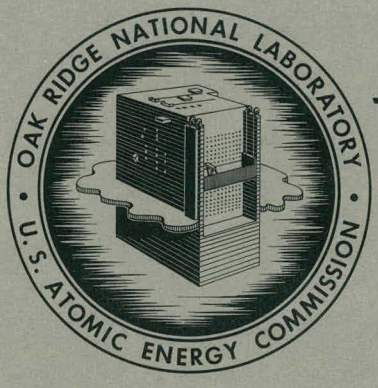

OAK RIDGE NATIONAL LABORATORY
operated by
UNION CARBIDE CORPORATION
for the
U.S. ATOMIC ENERGY COMMISSION

DISCLAIMER

Printed in USA. Price: $2.00 Available from the
Office of Technical Services
U. S. Department of Commerce
Washington 25, D. C.

ORNL-3551

A80032172

Contract No. W-7405-eng-26

Metals and Ceramics Division

CORROSION OF REFRACTORY METALS BY LITHIUM

James Richard DiStefano

Submitted as a thesis to the Graduate Council of the University of Tennessee in partial fulfillment of the requirements for the degree of Master of Science

MARCH 1964

OAK RIDGE NATIONAL LABORATORY
Oak Ridge, Tennessee
operated by
UNION CARBIDE CORPORATION
for the
U. S. ATOMIC ENERGY COMMISSION

ACKNOWLEDGMENTS

The author wishes to express his gratitude to his thesis advisor, Dr. E. E. Stansbury, for his advice during the course of this investigation and his help in the preparation of this manuscript.

A special note of thanks is extended to Mr. E. E. Hoffman for his many helpful suggestions during the course of this investigation and under whose direction this research was carried out. In addition, the author wishes to express his gratitude to Drs. J. V. Cathcart and R. E. Pawel of the Metals and Ceramics Division for their interest and assistance during the progress of this work and their help in the review of the manuscript.

Special thanks are extended to Mr. W. C. Thurber of the Metals and Ceramics Division for his constructive appraisal of the experimental work in this report and for his help in the preparation of the manuscript. The author is also indebted to Mr. J. H. DeVan who assisted in the review of this manuscript.

The author was fortunate in having been able to perform the experimental work at the Oak Ridge National Laboratory since this allowed him access to facilities, equipment, and personnel that were of invaluable assistance. Although it would be impossible to acknowledge all who contributed to this research, the author would like to thank, in particular, the following groups and individuals for their assistance:

Materials Compatibility Laboratory and especially D. H. Jansen and R. E. Potter.

The Metallography Group of the Metals and Ceramics Division and especially E. D. Bolling, L. G. Shrader, and R. S. Crouse.

R. M. Steele of the X-Ray Group of the Metals and Ceramics Division.

The Mechanical Properties Group of the Metals and Ceramics Division and especially C. W. Dollins of that group.

The Physical Metallurgy Group of the Metals and Ceramics Division and especially J. F. Newsome.

The Analytical Chemistry Division and especially W. R. Laing and H. G. Davis.

The Graphic Arts Department and in particular W. C. Colwell.

Mrs. Geneva Harris of the Metals and Ceramics Division Reports Office for the typing and preparation of the material for reproduction.

The author would like to express his gratitude to the Union Carbide Corporation, Nuclear Division, for its educational assistance program and to the High-Temperature Materials Program which provided financial support for this work.

TABLE OF CONTENTS

LIST OF TABLES

LIST OF FIGURES

CHAPTER I

SUMMARY

The pure metals niobium, tantalum, vanadium, titanium, and zirconium exhibit excellent resistance to dissolutive attack by lithium at temperatures even in excess of 800°C. However, the presence of small quantities of oxygen in either niobium or tantalum can cause the rapid penetration of these metals by lithium over a wide range of temperatures. Vanadium, titanium, and zirconium, on the other hand, do not show this susceptibility to lithium penetration even at oxygen concentrations in excess of 2000 parts per million.

Penetration of niobium or tantalum by lithium results in the formation of a complex corrosion product in grain boundaries or along certain crystallographic planes. This reduces both the tensile strength and ductility of niobium.

Oxygen was gettered from niobium, tantalum, and vanadium by lithium in all the tests. In the case of titanium and zirconium, oxygen redistribution occurred; but the direction, from solid metal to liquid metal or vice versa, depended on initial concentrations in the solid and liquid metal.

At oxygen concentrations above 500 parts per million, temperature and grain size were the most significant variables affecting depth of penetration. Low temperatures and large grain size favored penetration along certain crystallographic planes while high temperature and small grain size favored grain-boundary attack. In tests with

single crystals, penetration was observed to decrease with increased temperature. This was shown to be related to the rate at which oxygen diffused out of the niobium and was gettered by the lithium. Other variables such as time, heat treatment, prior deformation, and lithium purity were also investigated but were not found to be significant in the corrosion process.

Possible solutions to this problem were afforded by the addition of alloying elements to niobium. It was shown that the addition of zirconium could be effective in eliminating lithium penetration. Alloys heat treated such that oxygen was tied up as the compound ZrO_2 did not corrode. Vanadium, on the other hand, was not effective in providing corrosion protection, presumably because it does not preferentially tie up oxygen present in the alloy.

CHAPTER II

INTRODUCTION

In reactor systems requiring that a large amount of heat be removed from a relatively small volume, it is often necessary that a liquid metal be considered as the heat-transfer medium. Some liquid metals have many of the desirable physical and nuclear properties needed in a coolant to be used for this type of application, such as: (1) low melting point, (2) high boiling point, (3) low vapor pressure, (4) high heat capacity, (5) high thermal conductivity, (6) low density, (7) low viscosity, and (8) low neutron absorption cross section. One of the liquid metals that has been considered is lithium because it possesses a good combination of these properties. However, a serious problem which has limited its use is the severe corrosion which has been encountered in systems operating at high temperatures. In the early 1950's some preliminary studies (1,2) indicated that niobium and other refractory metals* were more resistant to liquid-metal corrosion than the previously tested conventional materials and alloys. In addition, their high melting points and potentiality for high strength at elevated temperatures made them excellent prospects for high-temperature reactor systems. Therefore, further investigation of the compatibility of refractory metal–lithium systems was begun.

---

*In this report, those metals in Groups 4A, 5A, and 6A of the Periodic Table are considered as refractory metals.

Studies of the interactions between liquid and solid metals have led authors (3–7) to classify the various types of phenomena that have been observed. One such classification (8) was given for refractory metal–alkali metal systems as follows:

I. Dissolutive corrosion mechanisms.
   A. Dissolution of solid metal by liquid metal.
   B. Dissimilar-metal mass transfer.
   C. Temperature-gradient mass transfer.
II. Impurity reaction mechanisms.
   A. Liquid-metal impurities.
   B. Solid-metal impurities.
   C. Partitioning of impurities between solid and liquid metal.

Although the early investigations indicated good resistance of the refractory metals to dissolutive attack by lithium (Mechanism 1), later tests showed that impurities in the system can deleteriously affect the corrosion behavior of these materials (Mechanism 2). Reactions by which compounds or complexes of the impurity with the solid metal and/or liquid metal are formed can cause a deterioration in properties of the solid metal. In addition, when an element such as oxygen is in solution in both the solid and liquid metal, then it will redistribute itself until it has the same chemical potential in each phase. At a particular temperature, the equilibrium ratio of the concentration of oxygen to be found in each phase should be constant and can be calculated from an expression* such as the following:

---

*See Appendix A for derivation.

$$\frac{C_B}{C_A} = \exp\left[\frac{\Delta F^{\circ}_{f(\text{A oxide})} - AF^{\circ}_{f(\text{B oxide})}}{RT}\right]\frac{(C_B)_s}{(C_A)_s}$$

where

C_A = concentration of solute in phase A,

C_B = concentration of solute in phase B,

$\Delta F^{\circ}_{f(\text{A oxide})}$ = standard free energy of formation of the oxide of A which can be in equilibrium with a solution of oxygen in A,

$\Delta F^{\circ}_{f(\text{B oxide})}$ = standard free energy of formation of the oxide of B which can be in equilibrium with a solution of oxygen in B,

$(C_B)_s$ = solubility of oxygen in B,

$(C_A)_s$ = solubility of oxygen in A.

At 500 and 800°C the following ratios were calculated from this equation.

System	$\frac{C_{\text{oxygen in solid metal}}}{C_{\text{oxygen in lithium}}}$ 500°C	800°C
Niobium-oxygen-lithium	5×10^{-11}	1×10^{-7}
Tantalum-oxygen-lithium	3×10^{-11}	3×10^{-8}
Vanadium-oxygen-lithium	7×10^{-11}	3×10^{-9}
Titanium-oxygen-lithium	5×10^{-2}	2×10^{-2}
Zirconium-oxygen-lithium	3	4

Although, as discussed in Appendix A, these values may be incorrect by several orders of magnitude, they do indicate that lithium should getter most of the oxygen present in niobium, tantalum, or vanadium.

Titanium and zirconium, on the other hand, will either gain or lose oxygen in lithium depending on the initial concentrations present in each.

CHAPTER III

OBJECTIVE OF THE STUDY

The purpose of this study was to investigate more thoroughly the role of impurities in determining the compatibility of refractory metal–lithium systems, the primary objective being to understand the mechanism by which corrosion occurs. In addition, methods by which the corrosion resistance of these potential reactor materials to lithium could be improved also were sought.

In order to determine the principal variables affecting corrosion in the niobium-oxygen-lithium system, the following were determined:

1. Effect of oxygen, nitrogen, and carbon in niobium.
2. Effect of temperature.
3. Effect of time.
4. Effect of grain size.
5. Effect of heat treatment.
6. Effect of deformation.
7. Effect of lithium purity.
8. Effect of alloying additions.

It was hoped that from an evaluation of the effect of these variables, even if the mechanism by which corrosion occurs could not be completely defined, a better understanding of the nature of the corrosion processes might be gained.

CHAPTER IV

REVIEW OF PREVIOUS EXPERIMENTS

Static corrosion test data (1) and solubility studies (2,9) indicated the refractory metals to be more resistant to dissolutive corrosion than the more common metals and alloys. In addition, extensive studies of corrosion by lithium conducted in both static and dynamic test systems showed that only the refractory metals are suitable for application in dynamic, nonisothermal systems operating at temperatures in excess of 650°C (10). Results of these early studies are summarized in bar graph form in Figure 1.

Because of its availability and good fabricability, niobium was selected for further study since, as shown in Figure 1, it apparently also possessed good resistance to attack by lithium at elevated temperatures. However, some later tests showed that under certain conditions lithium penetration could occur. One such example was a natural circulation loop test conducted at 871°C (1600°F) for 23 hours. Metallographic examination of various sections of the test system revealed general attack in welded regions and a more random type of corrosion in certain areas of the base material. A typical example of the random attack observed is illustrated in Figure 2. The full extent of penetration, especially in nonwelded regions, was not discovered until cross sections from the loop were polished and allowed to age in air for several days at room temperature. The specimen surface became stained, as shown in Figure 3, when lithium in the corroded areas

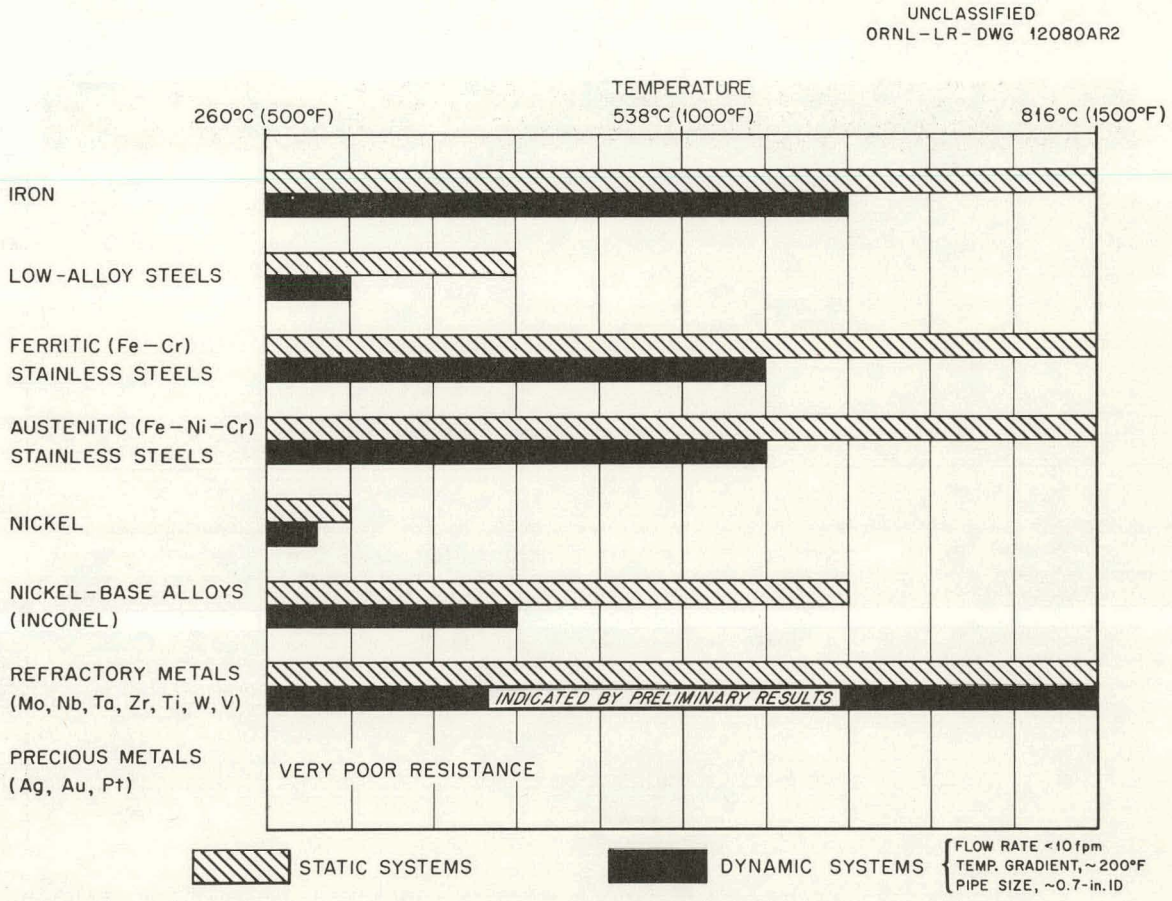

Figure 1. Corrosion resistance of various metals and alloys to lithium.

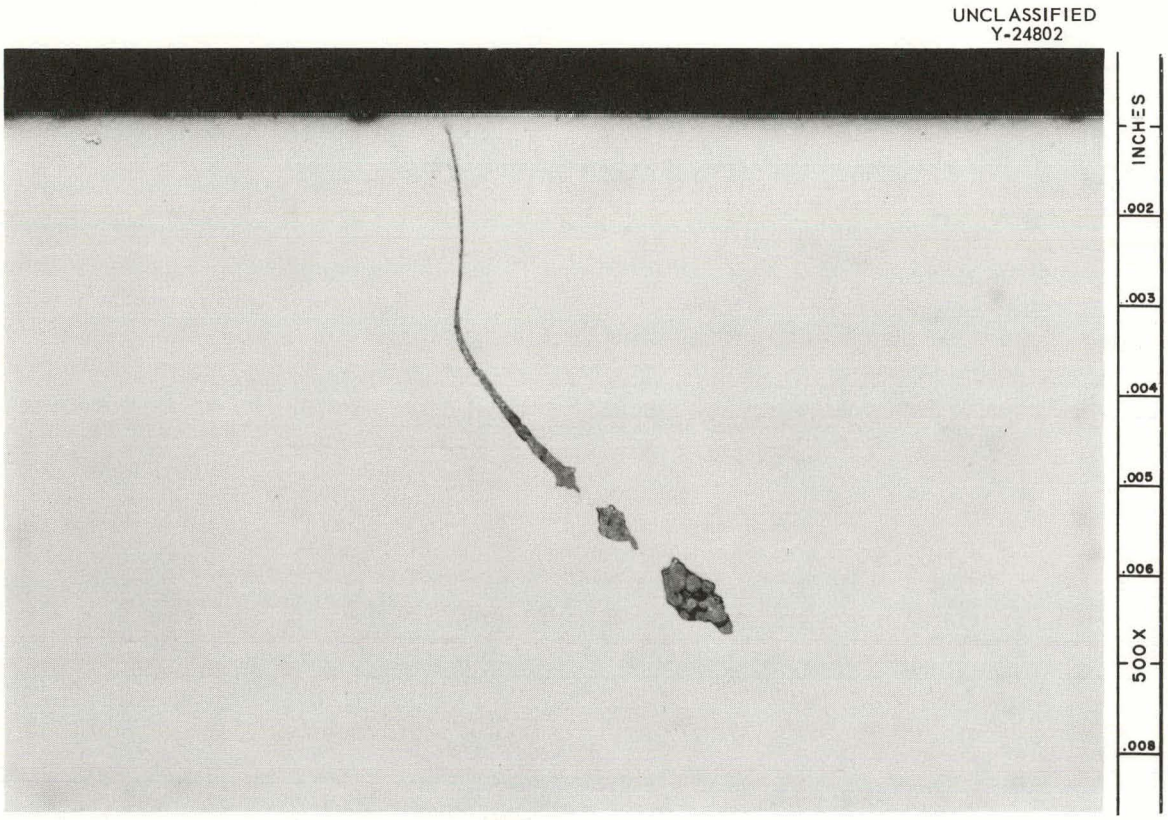

Figure 2. Example of random attack observed in niobium exposed to lithium for 23 hours at 871°C. As-polished. Reduced 6%.

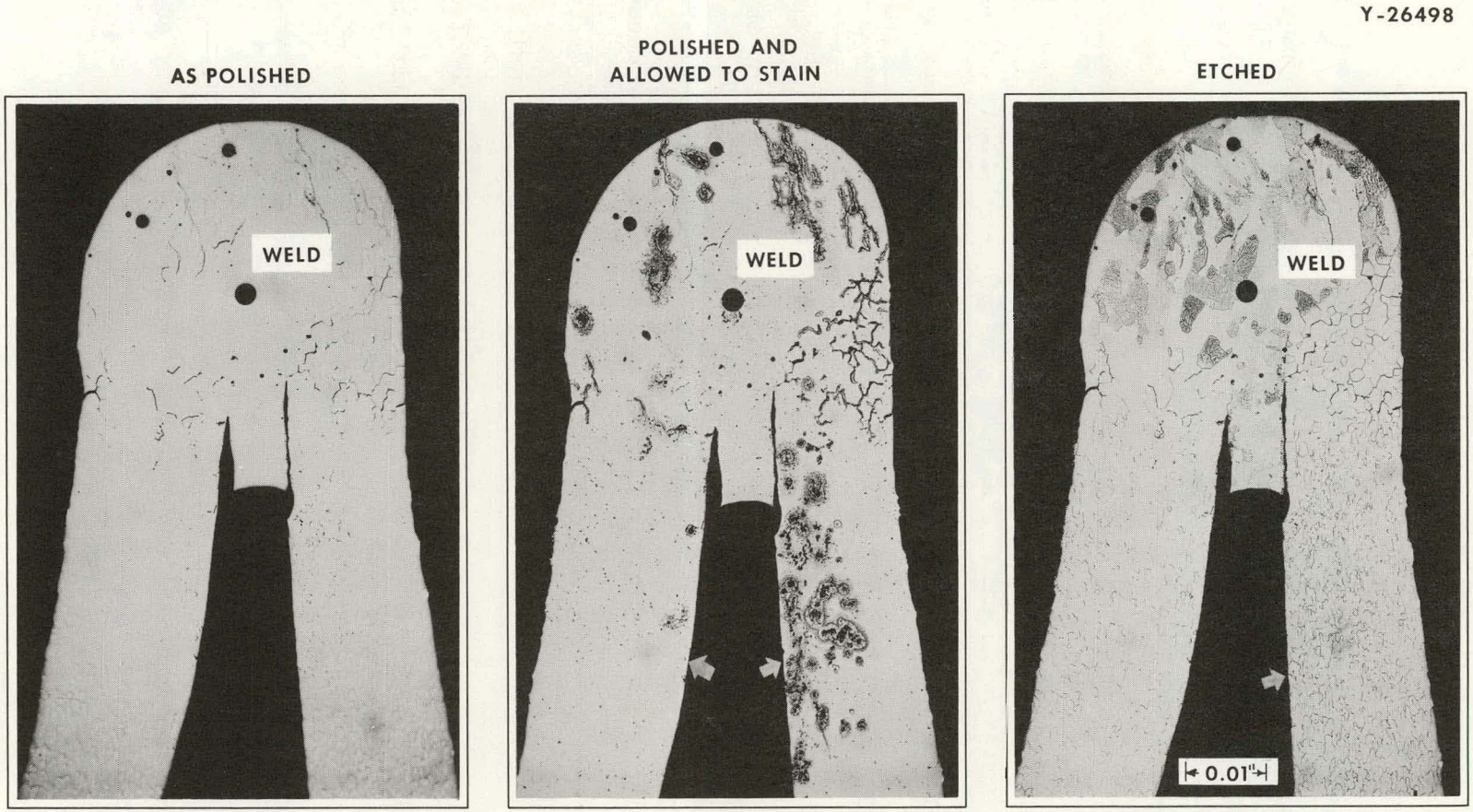

Figure 3. Tube wall and weld region of niobium loop in which lithium was circulated for 23 hours at 871°C. Arrows indicate the surfaces exposed to lithium.

reacted with moisture in the air. The corrosion observed metallographically was verified by chemical analysis to be associated with lithium penetration. Analysis of turnings machined from a section taken from the niobium test loop showed a lithium concentration gradient in the tube wall that was in agreement with metallographic observations of corrosion.

Further studies by Hoffman (11), to determine the reason for this corrosion behavior, demonstrated that the oxygen concentration in niobium was a principal variable determining the amount of penetration. It was previously pointed out that, although attack by lithium appeared to be random, it did occur more often in welds and other areas subject to contamination by gaseous impurities such as oxygen or nitrogen. It was found, as shown in Figure 4, that the addition of 0.134 per cent nitrogen to niobium did not affect the corrosion resistance of the niobium, but very severe corrosion occurred when 0.527 per cent oxygen was added. Hoffman further demonstrated that the amount of lithium penetration increased with increasing oxygen in the niobium (Figure 5). Although no specific mechanism for the corrosion process was proposed, it was suggested that lithium penetration could have occurred if oxygen segregation in the niobium resulted in the formation of niobium oxide in the grain boundaries and this phase were reduced by lithium.

Based on these preliminary data, a more detailed study of this phenomenon was undertaken. The major portion of the current

UNCLASSIFIED
ORNL-LR-DWG 34982

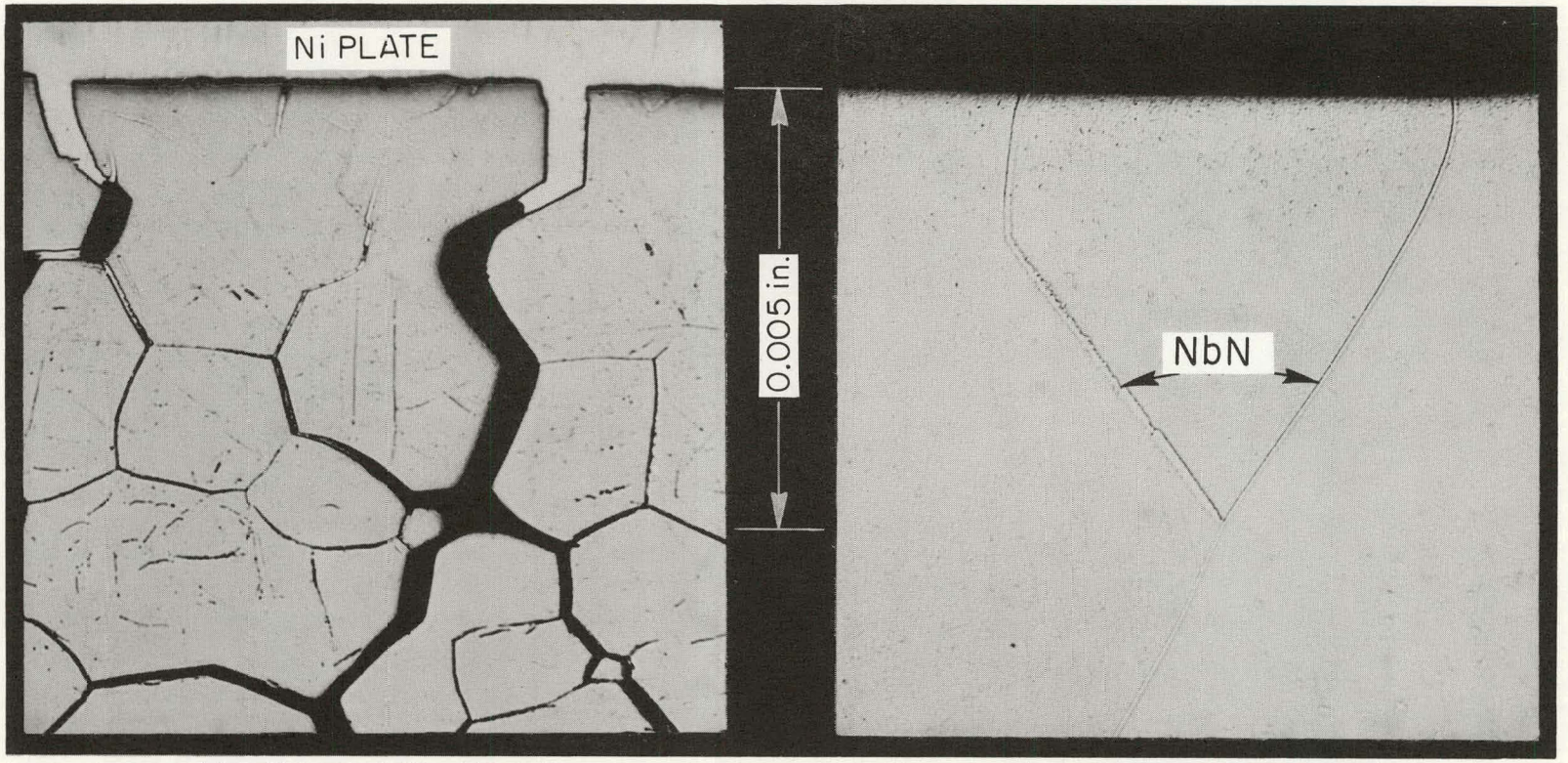

(AS POLISHED-500X)

(a) 0.527 % O_2 ADDED PRIOR TO WELDING

(AS POLISHED-500X)

(b) 0.134 % N_2 ADDED PRIOR TO WELDING

Figure 4. Weld zones of niobium specimens following exposure to lithium for 100 hours at 816°C. As-polished. Reduced 9%.

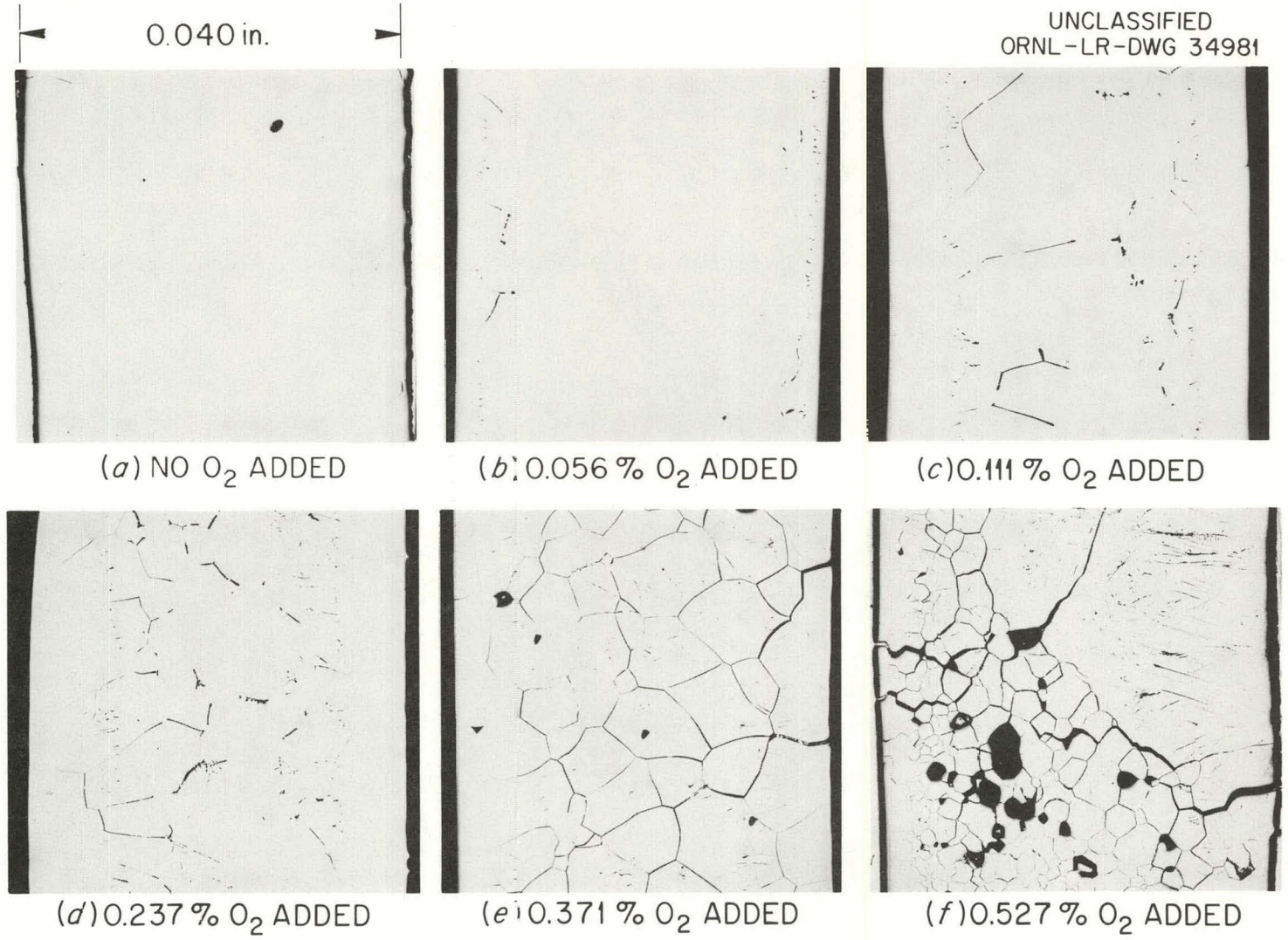

Figure 5. Weld zones of oxygen-contaminated niobium specimens after exposure to lithium for 100 hours at 816°C. As-polished.

investigation deals with niobium and niobium alloys with some cursory work reported on tantalum, vanadium, titanium, and zirconium.

CHAPTER V

EXPERIMENTAL PROCEDURE

Materials

Lithium used in these studies was a low-chloride grade obtained from the Foote Mineral Company. A typical analysis of this material, as specified by the manufacturer, is listed in Table I. Purification procedures as described in the literature (12) were used to reduce the oxygen concentration from approximately 2000 parts per million to 100–200 parts per million and the nitrogen content from approximately 3000 parts per million to less than 20 parts per million. The sequence of steps taken to purify the lithium consisted of (1) filtration at 250°C through a stainless steel filter with a 10-micron pore size to reduce gross amounts of nitrogen and oxygen contamination, (2) gettering with titanium sponge for 24 hours at 800°C to reduce the nitrogen concentration to less than 100 parts per million, and (3) cold trapping for 100 hours to reduce the oxygen concentration to the 100–200 parts per million range. Nitrogen was determined by the method described by White (13) and Sax (14), and oxygen was determined by activation analysis (15). Good reproducibility was found in determining nitrogen, but considerable scatter was observed in oxygen analysis.

The refractory-metal samples were obtained from high-purity electron-beam-melted stock. A typical chemical analysis of a heat of niobium is given in Table II. Metal impurities were determined using spectrographic techniques and gaseous impurities by vacuum fusion (16).

TABLE I

TYPICAL LITHIUM PURITY AS SPECIFIED BY THE MANUFACTURER

Element	Concentration (%)
Lithium	99.88
Sodium	0.015–0.016
Potassium	0.06–0.07
Calcium	0.0001
Iron	0.0005
Aluminum	0.0005
Silicon	0.001
Chlorine	0.04
Nitrogen	0.012

TABLE II

ANALYSIS OF TYPICAL HEAT OF NIOBIUM

Element	Concentration (%)
Iron	< 0.01
Silicon	< 0.01
Titanium	< 0.015
Tantalum	0.076
Zirconium	< 0.1
Boron	< 0.0001
Hydrogen	< 0.0001
Carbon	0.005
Nitrogen	0.006
Oxygen	0.016

Polycrystalline specimens were usually obtained from cold-rolled sheet. These were deburred after cutting, degreased with acetone or other suitable solvents, and then vacuum annealed at temperatures from 1000 to 1600°C. Single-crystal specimens were cut from electron-beam-melted ingots and then either mechanically polished or electropolished to produce a suitable surface finish. During the course of this investigation, specimens having various surface finishes were tested but the results indicated that this was not a significant variable in the corrosion process.

Procedure

Individual additions of oxygen, nitrogen, and carbon were made to the solid metal in order to evaluate the effect of these impurities on corrosion. Oxygen or nitrogen, in gaseous form, was added at 1000°C and 1×10^{-4} torr in the apparatus shown schematically in Figure 6. The reaction chamber consisted of a mullite combustion tube 2 inches in diameter and 36 inches long. An electric resistance furnace using silicon carbide elements surrounded the mullite reaction tube and was capable of operation up to about 1300°C. Inside the reaction tube, the niobium specimen was contained in a quartz cylinder, open to the downstream end of the oxygen flow and having numerous one-eighth-inch diameter holes in its lateral surface. This design was found to result in a more uniform oxygen pickup in specimens longer than one-half inch. The quartz container and specimen were moved in and out of the constant temperature hot zone of the furnace with a

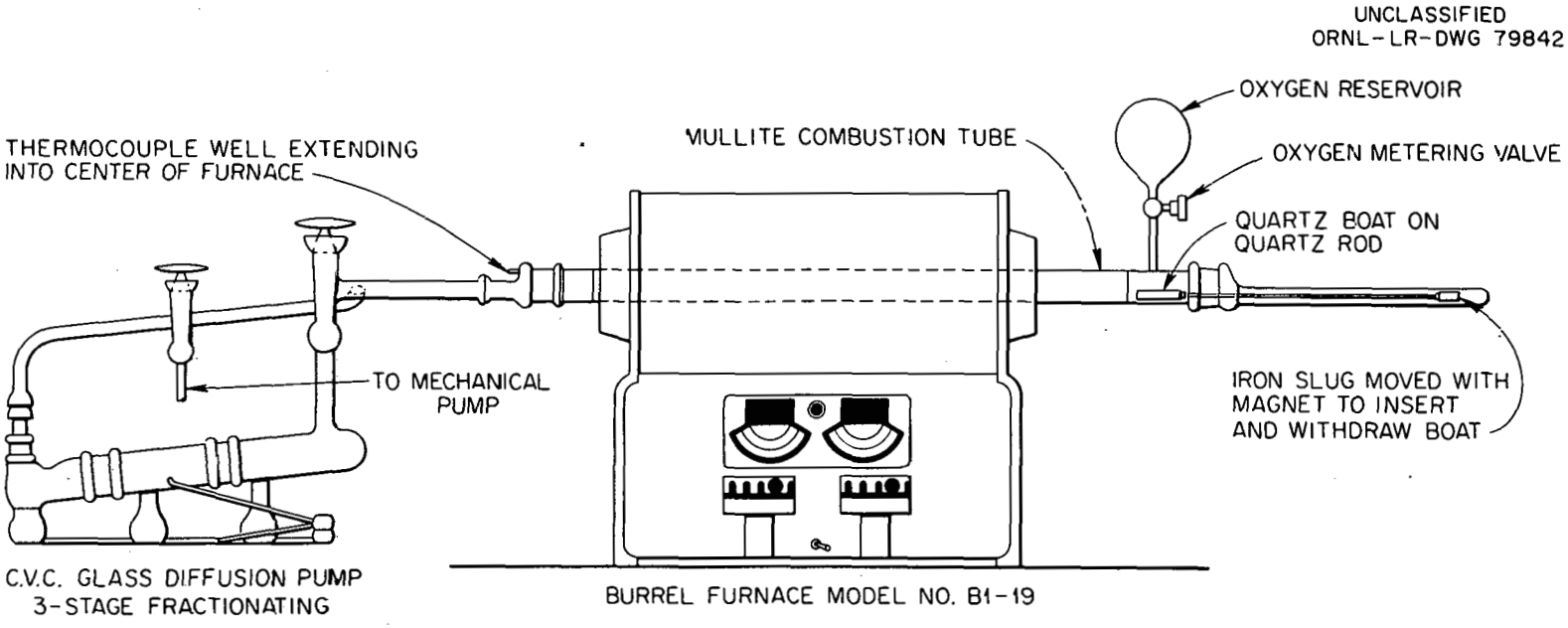

Figure 6. Schematic drawing of system used to add oxygen or nitrogen to refractory metals.

magnet which moved an iron slug attached to the quartz cylinder. Times of 15 minutes up to several hours were required to provide the desired oxygen concentrations. Evacuation of the system was accomplished by a Welch Duo Seal mechanical pump and a three-stage oil diffusion pump, Model GF-25 from Consolidated Vacuum Corporation, in which Octoil S diffusion pump oil was used. The oxygen (or nitrogen) pressure in the combustion tube was controlled by manual operation of a metering valve. Tank oxygen (99.5 per cent minimum purity) was used as the oxygen source, and tank nitrogen as the nitrogen source. The specimen temperature was measured by a platinum versus platinum–10 per cent rhodium thermocouple placed in a thermocouple well which extended into the constant temperature zone of the furnace. The temperature of the furnace was controlled by a platinum versus platinum–10 per cent rhodium thermocouple attached to the outside of the mullite combustion tube in the constant temperature zone and connected to a Wheelco control system.

Unless otherwise indicated, each specimen was homogenized after oxidation for 2 hours at 1300°C to ensure more random distribution of the element. The amount of each addition was measured by weight change in the sample after oxidation as well as by chemical analysis, and good correlation was generally found. In order to determine the homogeneity of specimens to which oxygen had been added, a relation between oxygen concentration and hardness of niobium was determined as shown in Figure 7. Hardness was then used as a measure of the oxygen concentration in niobium, and the oxygen distribution before and after

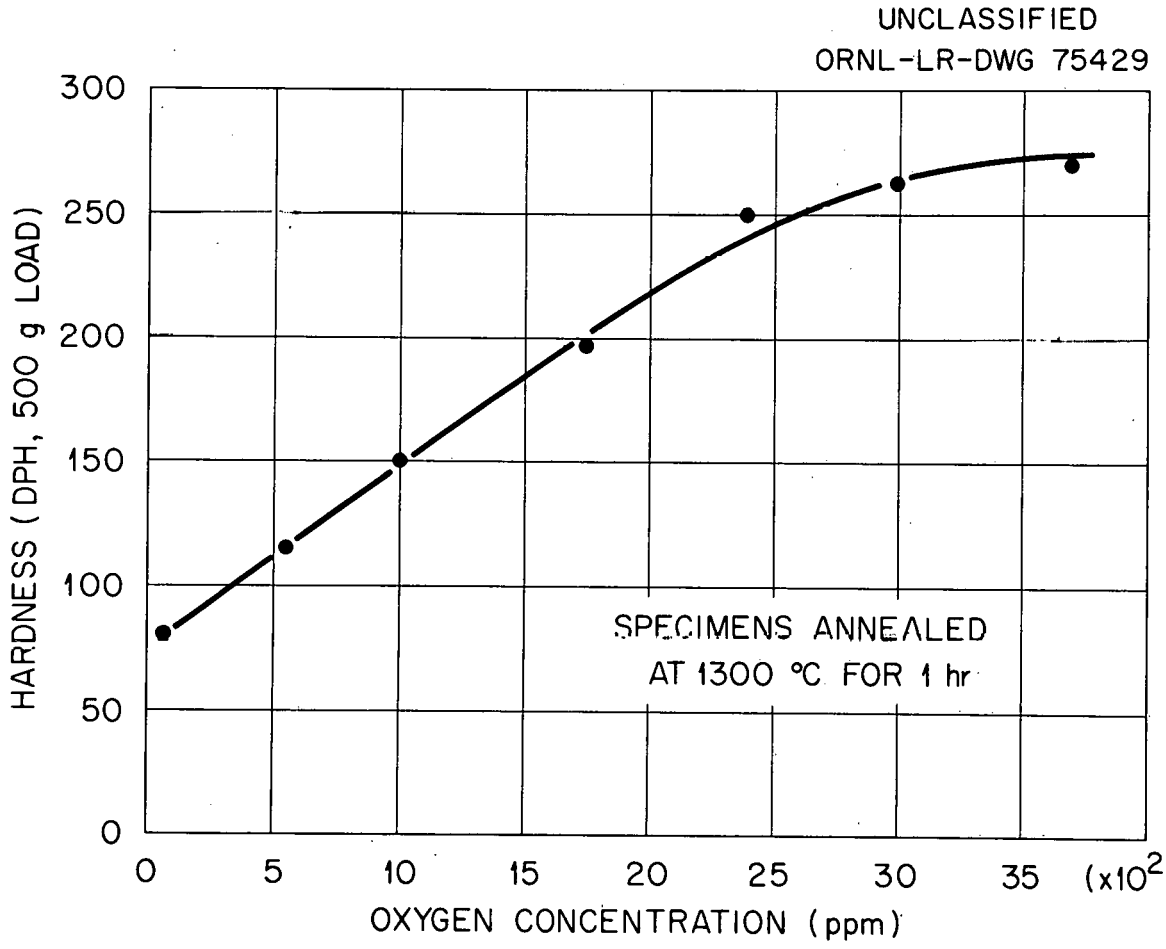

Figure 7. Hardness of niobium as a function of oxygen concentration.

homogenization at 1300°C was determined as shown in Figure 8. It can be seen that the homogenization treatment produced a uniform oxygen distribution.

The method for adding carbon to niobium involved electron-beam-melting niobium and various amounts of niobium carbide. The alloys were subsequently cold rolled to sheet and annealed at 1400°C for 2 hours.

Corrosion testing was performed in an assembly maintained in a stationary position at a controlled constant temperature. The test system, shown schematically in Figure 9, consisted of a refractory-metal specimen in a capsule of the same refractory metal. An additional outer capsule was used to protect the refractory metal from oxidation during test.

Because of the extreme reactivity of lithium in air, it was handled under vacuum or in an inert-gas atmosphere at all times. The atmosphere chamber shown in Figure 10 was used to open the lithium container and to melt and cast it into "stick" molds for loading into the refractory-metal capsule. It was also used to weld the test assemblies since refractory metals can become contaminated when welded in environments containing oxygen and nitrogen.

In the early stages of this investigation, the test system as shown in Figure 9 was placed in a furnace already being maintained at the test temperature. However, because of the extreme rapidity of the corrosion process, it became necessary to restrict the specimen to the opposite end of the container from the lithium until the entire system

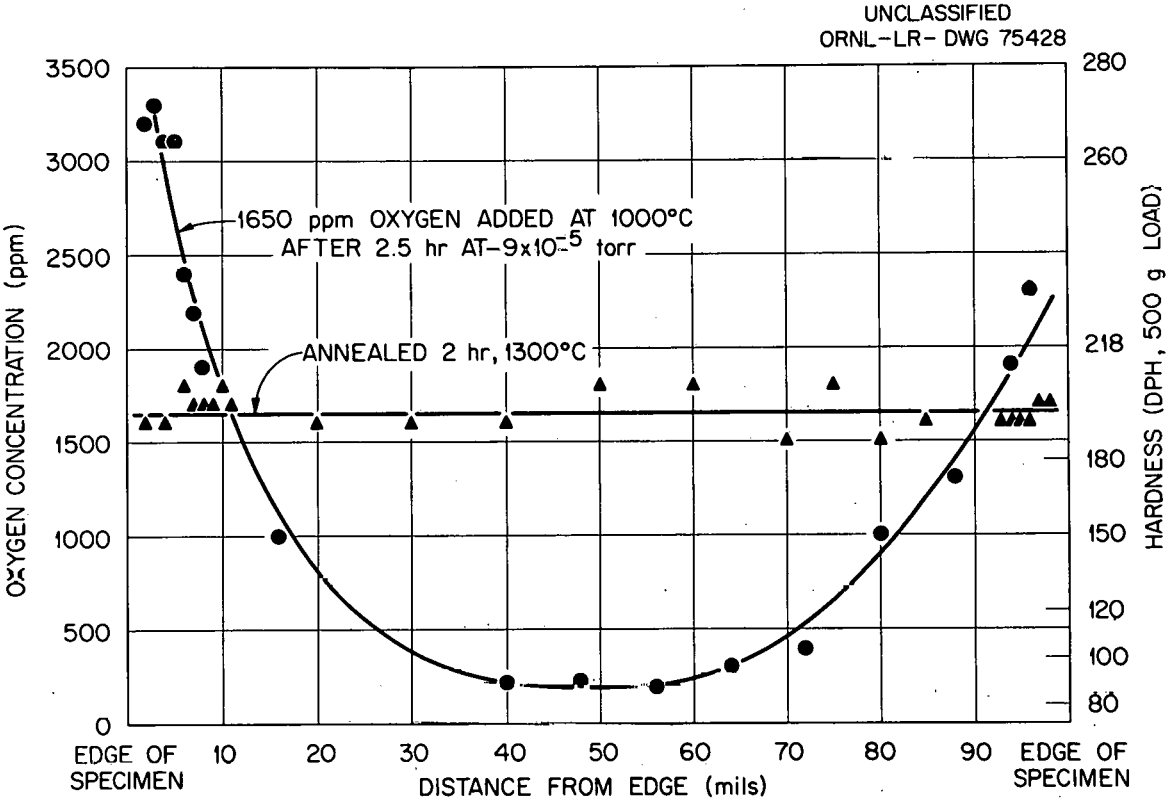

Figure 8. Oxygen distribution in niobium after oxidation at 1000°C and oxidation followed by annealing 2 hours at 1300°C.

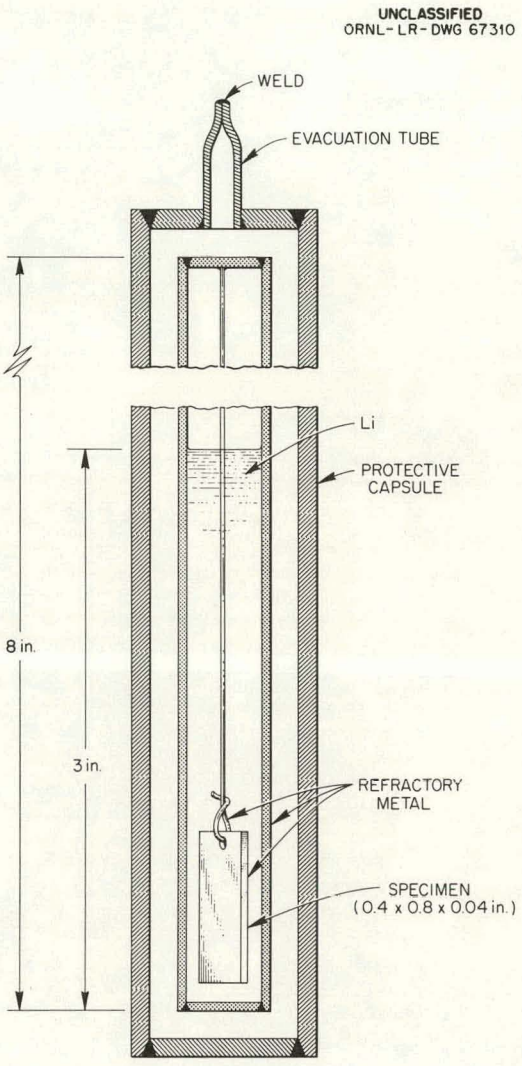

Figure 9. Typical refractory metal—lithium corrosion test system.

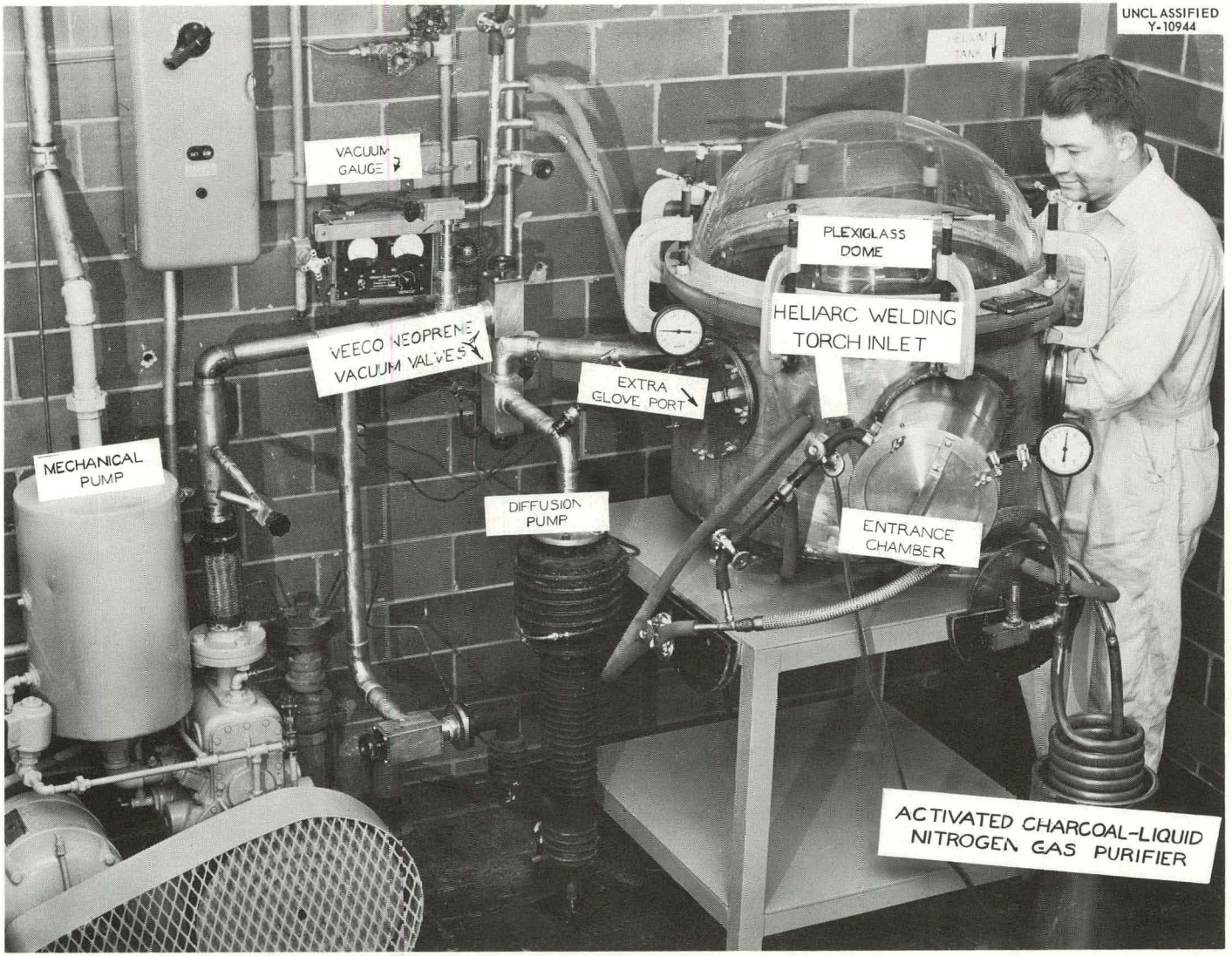

Figure 10. Inert-atmosphere chamber.

was at the test temperature. The container was then quickly inverted to allow liquid lithium to contact the specimen. During the test, the temperature was controlled by a Brown Pyr-O-Vane type controller and was recorded on a multipoint recorder. The maximum temperature variation was ±10°C. To terminate the test the container was again inverted and quenched in oil. The capsule was cut open in the atmosphere chamber and any lithium remaining on the specimen surface was removed either by distillation under vacuum at 700°C or by immersion in alcohol.

Evaluation

The methods used to determine the extent and nature of lithium penetration included weight change, dimensional change, chemical analysis, x-ray analysis, mechanical properties change, hardness change, and metallography.

Weight Change. Weight determinations were made on specimens before and after test. These data did not prove useful in determining the amount of lithium penetration since both lithium increase and oxygen decrease in niobium generally occurred.

Dimensional Change. Specimen dimensional changes were determined by micrometer measurements but were too small to be of value in evaluating the extent of corrosion.

Chemical Analysis.* Chemical analyses of specimens before and after test were useful in determining the amount of lithium pickup which had occurred as well as the amount of oxygen that had been gettered by the lithium.

X-Ray Analysis. X-ray diffraction methods were used to determine crystal orientations, and to identify surface layers which sometimes formed on the niobium. It was also used in an unsuccessful attempt to identify the corrosion product which formed in the niobium-oxygen-lithium system.

Mechanical Properties Change. To determine the effect of corrosion on the mechanical properties of niobium, its room-temperature tensile strength and per cent elongation were measured before and after exposure to lithium. Subsize specimens, die-punched from niobium sheet and having a gage-length-to-width ratio of eight, were used for this purpose. Data reported are a result of duplicate tests and a correlation between depth of attack and corrosion was found.

Hardness Change. Microhardness measurements were useful in evaluating the rate of oxygen removal from the niobium. Changes in hardness were found to be important in explaining the effects of some

---

*All chemical analyses were performed by the Analytical Chemistry Division, Oak Ridge National Laboratory, unless otherwise indicated. All concentrations are reported as per cent or parts per million by weight.

variables such as temperature and grain size on the corrosion process. Hardness measurements reported are the average of three or more determinations for each point plotted.

Metallography. Metallographic methods were by far the most useful in determining the amount of lithium penetration. The method for polishing refractory-metal specimens was that reported by Gray and Long (17). Careful techniques were required because of the sensitivity of the corrosion product to polishing and etching. Because of the brittleness of the corrosion product, corrosion along grain boundaries often caused grains to become dislodged during polishing. Grain-boundary corrosion effects were generally observable in specimens in the as-polished condition. Transgranular attack, on the other hand, often could not be detected until the specimen was etched.

CHAPTER VI

RESULTS AND DISCUSSION

I. UNALLOYED NIOBIUM

Effect of Oxygen, Nitrogen, and Carbon

Individual additions of oxygen and nitrogen to niobium verified the general conclusion previously reported by Hoffman (18) that lithium penetration of niobium can be related to the initial oxygen concentration in the solid metal. Additions of up to 0.1 per cent carbon and 0.135 per cent nitrogen did not result in corrosion of niobium by lithium after 100 hours exposure at 816°C. These results are summarized in Table III which shows that oxygen in niobium is the principal interstitial impurity responsible for lithium attack.

In addition to the grain-boundary penetration reported by Hoffman (18), transgranular attack was also observed. In this case, corrosion occurred along a certain crystallographic plane (or planes), the corrosion product being in the form of platelets. Both types of penetration are illustrated in Figures 11 and 12. The depth to which the platelets extended into the metal also increased with increasing oxygen in the niobium as shown in Figure 12. In order to identify the habit plane of the corrosion product, a single crystal was polished on two faces having indices close to {110} and {100}. By successive steps of polishing and making x-ray photographs of these faces with the back-reflection Laue technique, crystal faces within 2 degrees of

TABLE III

DEPTH OF ATTACK AS A FUNCTION OF OXYGEN, NITROGEN, AND CARBON IN NIOBIUM EXPOSED TO LITHIUM FOR 100 HOURS AT 816 °C

Maximum Depth of Attack (mils)	Initial Concentration (ppm)		
	Oxygen	Nitrogen	Carbon
0	160	80	30
1	500	80	30
3	650	80	30
4	1000	80	30
10	1700	80	30
0	60	50	7
0	60	600	7
0	60	1350	7
0	40	60	500
0	40	60	1000

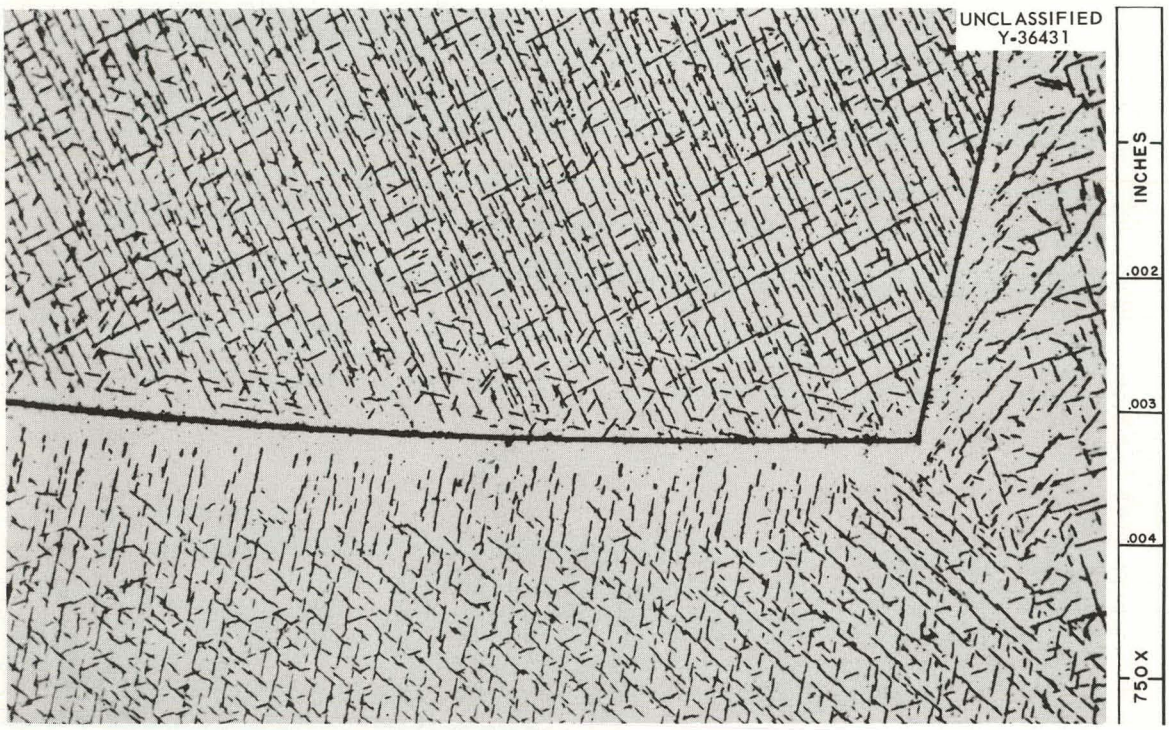

Figure 11. Transcrystalline and grain-boundary penetration of niobium containing 1500 parts per million oxygen and exposed to lithium for 100 hours at 500°C. Etchant: $HF-HNO_3-H_2SO_4-H_2O$. Reduced 7%.

UNCLASSIFIED
PHOTO 56128R

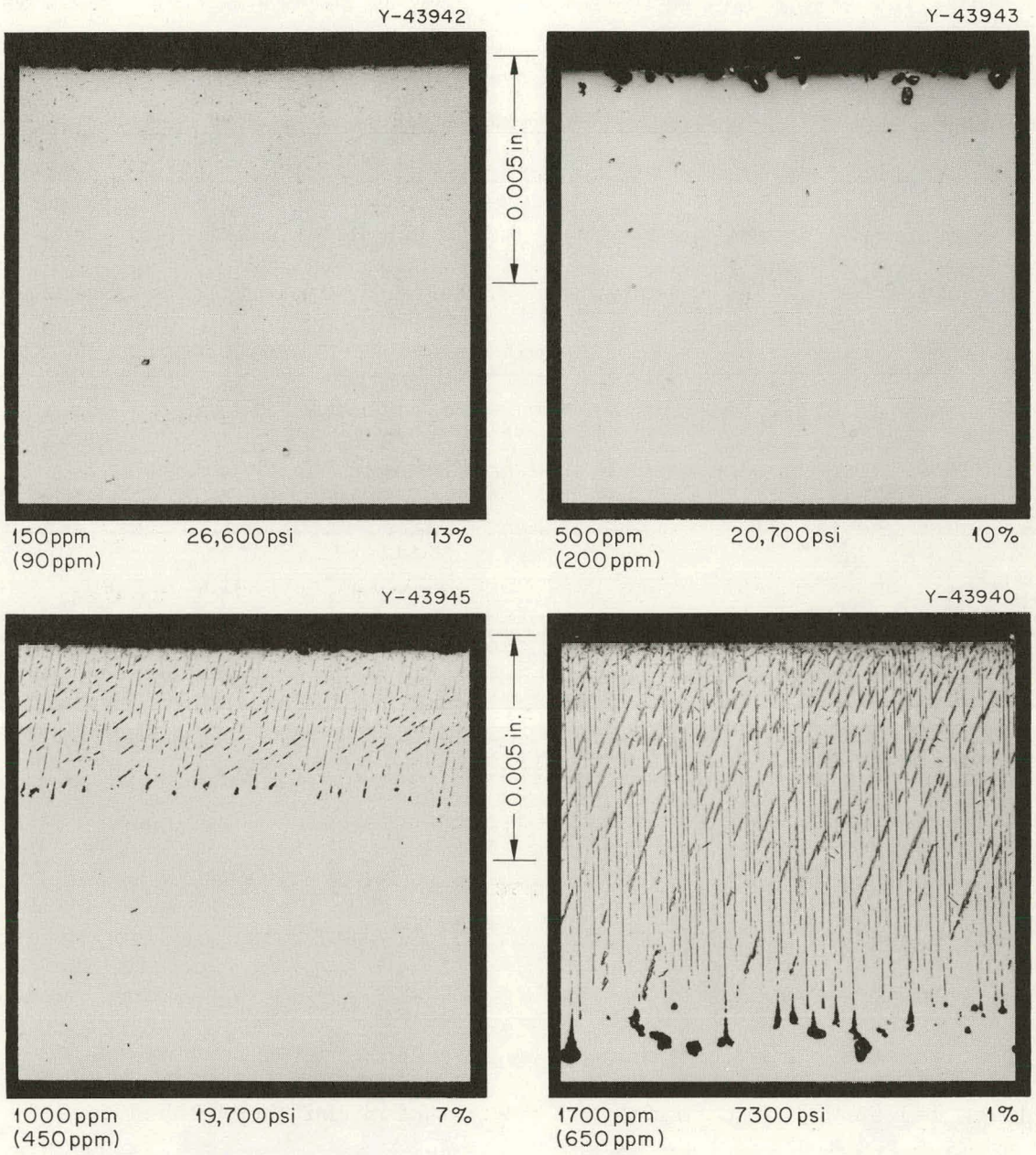

Figure 12. Effect of initial oxygen concentration, 150–1700 parts per million, in niobium on the depth of attack by lithium. Test conditions: 816°C for 100 hours. Following test, the room-temperature tensile strength varied from 26,600 to 7,300 pounds per square inch, the elongation in 2-inch gage length varied from 13 to 1 per cent, and the oxygen concentration varied from 90 to 650 parts per million. Etchant: $HF\text{-}HNO_3\text{-}H_2SO_4\text{-}H_2O$.

{110} and {100} were developed. The crystal was oxidized to 1000 parts per million oxygen and then tested in lithium for 5 hours at 500°C to produce a crystallographic corrosion pattern. Standard stereographic techniques were then used to identify the habit plane as {110}.

The effect of lithium penetration on the mechanical properties of niobium was investigated by measuring the tensile strength and elongation before and after exposure. After the addition of various amounts of oxygen, one set of specimens was heat treated in argon for 100 hours at 816°C and another set was exposed to lithium for 100 hours at 816°C. The results are plotted in Figure 13 which show that, although the tensile strength of heat-treated niobium increased and the per cent elongation remained constant with increasing oxygen, exposure to lithium resulted in a decrease in both tensile strength and elongation. This loss in strength and ductility increased with the depth of lithium penetration (Figure 12, page 33).

The small size and amount of the corrosion product made it difficult to recover sufficient amounts for quantitative analyses and hence prevented positive identification. It was found, however, that the solution used to etch the niobium (HF-HNO_3-H_2SO_4-H_2O) very rapidly dissolved the corrosion product. A corroded niobium specimen was distilled at 700°C to remove any free lithium and then etched in this solution. Analysis of the solution indicated that lithium was a component of the corrosion phase. In addition, chemical analyses (Figure 12, page 33) and hardness measurements (Figure 14) always indicated that the niobium lost oxygen during the exposure to lithium. However,

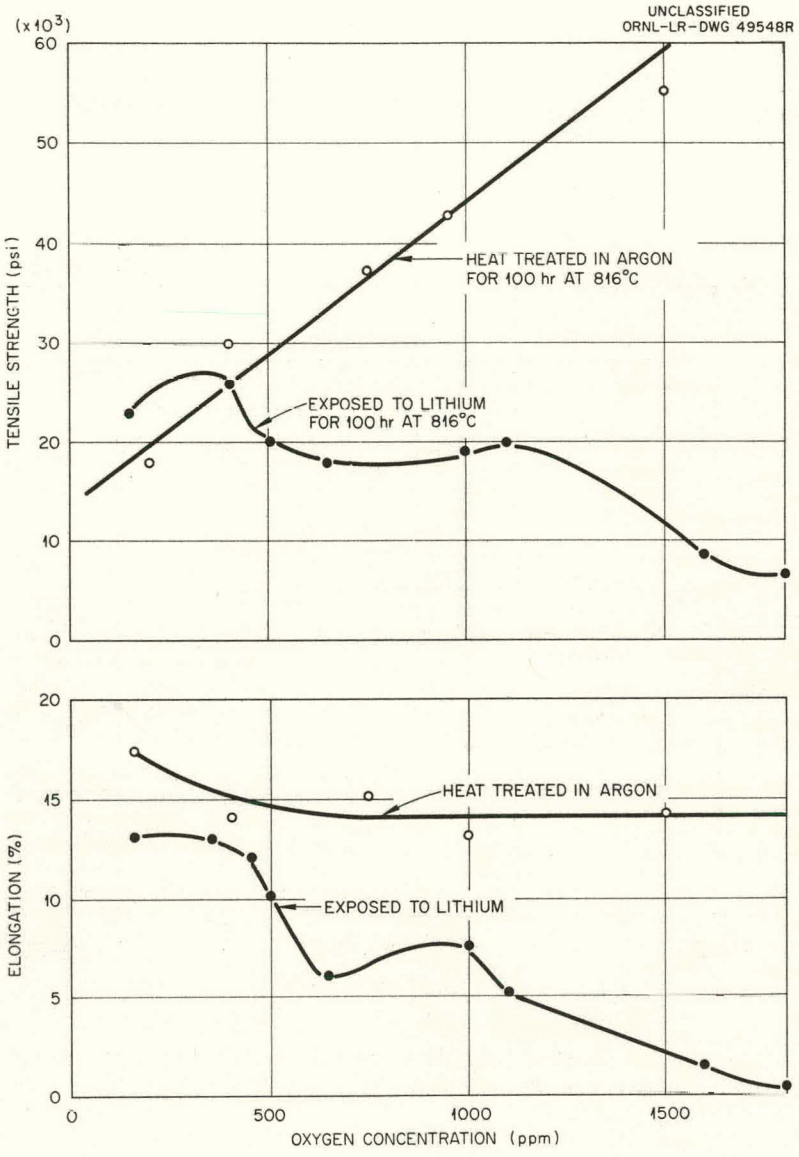

Figure 13. Effect of initial oxygen concentration on the mechanical properties of niobium following heat treatment in argon and exposure to lithium at 816°C. Specimen thickness: 0.040 inch.

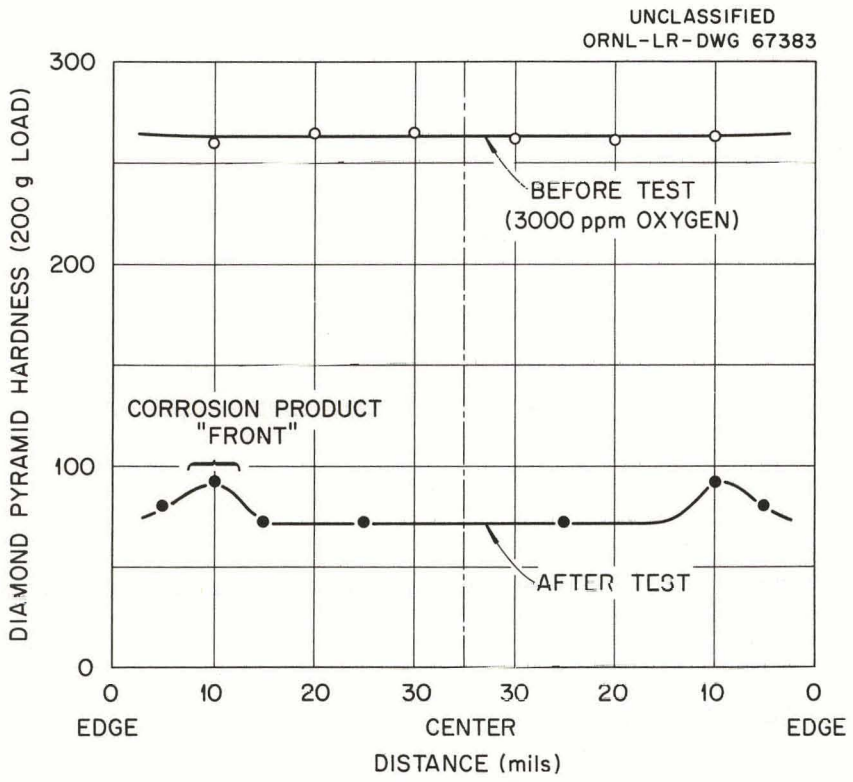

Figure 14. Hardness profile across niobium specimen before and after exposure to lithium for 100 hours at 816°C.

as shown in Figures 14, page 36, and 15, the area in the vicinity of the corrosion "front" exhibited a peak in hardness. In Figure 15 the hardness has been plotted on a photomicrograph of a cross section of the specimen referred to in Figure 14, page 36. When 0.010 inch was removed from each surface of this specimen, reanalysis showed a lower oxygen concentration than before this material was removed. (See Table VIII, page 69, for similar data on a series of specimens treated in this manner.) These data indicated that oxygen is also a component of the corrosion product. Some of the corrosion product from a specimen such as shown in Figure 16 was recovered and an x-ray pattern obtained. The diffraction lines were found to be consistent with a rhombohedral unit cell having hexagonal parameters a $\cong$ 7.49 A and c $\cong$ 7.97 A. This result was compared with data for Li_2O and Li_2O_2 but no similarity was found. Compounds* of various niobates of lithium such as $LiNbO_3$, $LiNbO_4$, and Li_2NbO_3 were then synthesized according to directions outlined in the literature (19–21) and x-ray patterns made. These were also compared with the pattern of the corrosion product, but again no close similarity was found. Thus, although it was concluded that the corrosion product was probably a lithium-niobium-oxygen compound, no positive identification could be made.

In addition to oxygen concentration, other test variables investigated were temperature, time, grain size, heat treatment, deformation,

---

*Compounds were made by Analytical Chemistry Division.

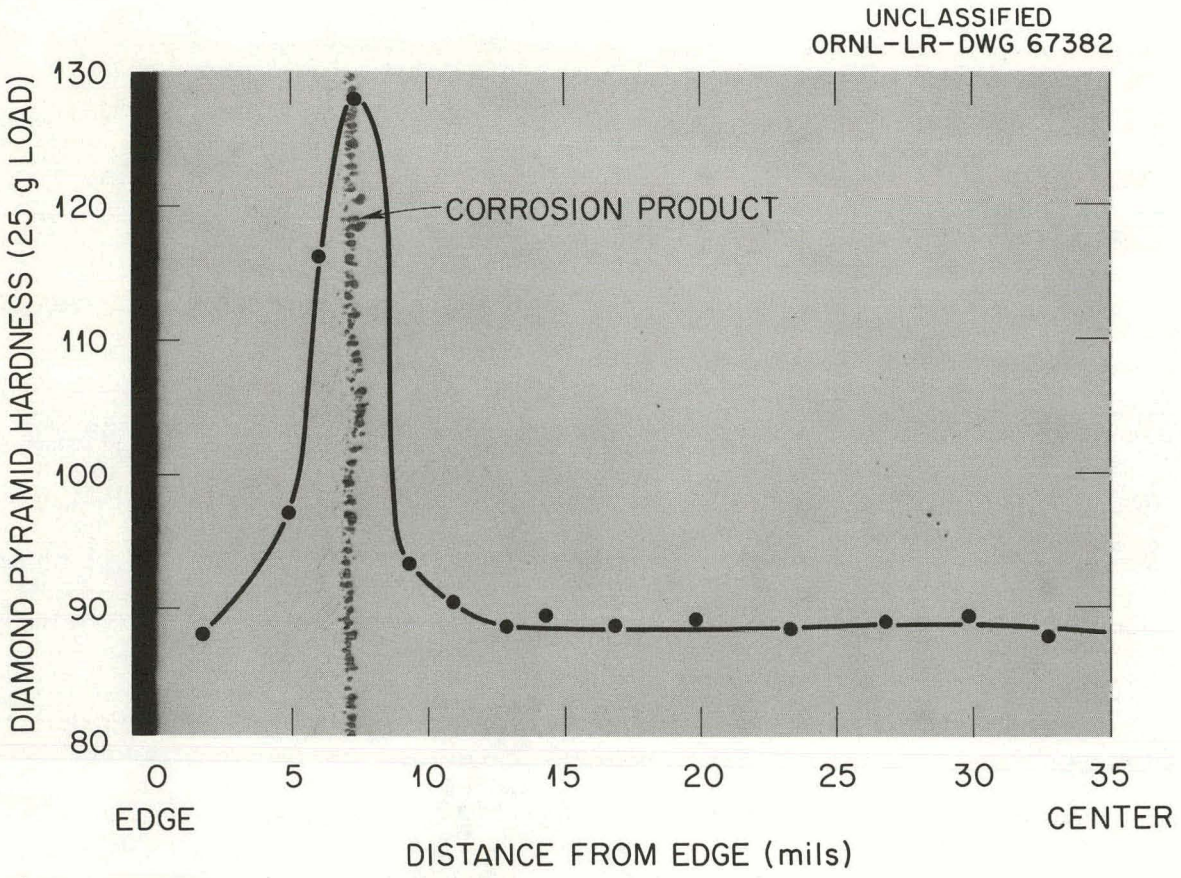

Figure 15. Microhardness profile across niobium specimen after exposure to lithium for 100 hours at 816°C. As-polished.

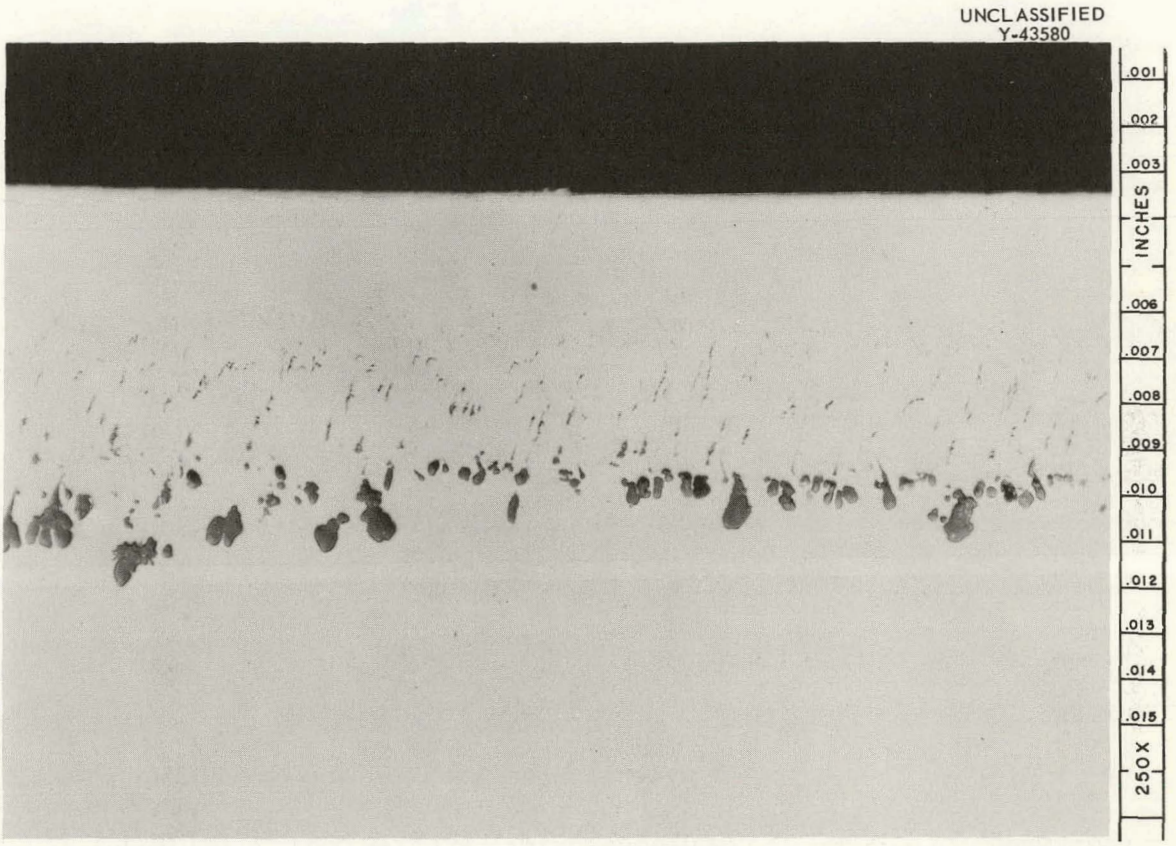

Figure 16. Niobium specimen from which corrosion product was obtained for x-ray analysis. As-polished. Reduced 5%.

and lithium purity. Although oxygen in niobium was found to be the controlling variable in the corrosion process, other variables were significant in determining the depth of lithium penetration at a constant initial oxygen concentration. If the oxygen concentration in niobium was less than a threshold value of approximately 400 parts per million, then, as shown in Table IV, lithium penetration did not occur under various test conditions. At concentrations above 500 parts per million oxygen, temperature was the most important additional variable.

Effect of Temperature

The effect of temperature on depth of penetration depends on initial oxygen concentration, time, grain size, and test procedure. These variables determine what sort of effect temperature will have because there are essentially two processes which occur when niobium is in contact with lithium: (1) lithium penetration and (2) oxygen redistribution. The process which has been discussed thus far is that of lithium penetration. However, since lithium penetration depends on the amount of oxygen in niobium, gettering of oxygen from niobium by lithium can affect the depth of penetration. Gettering is more important at high temperatures where oxygen diffusion rates in niobium are also high. The importance of oxygen removal can be shown by solution of Fick's law with the appropriate boundary conditions for oxygen diffusing out of niobium into the lithium. In Figure 17, a plot of the ratio of the oxygen concentration at a depth 0.005 inch from the

TABLE IV

LITHIUM PENETRATION OF NIOBIUM CONTAINING
≤ 500 PARTS PER MILLION OXYGEN

Initial Oxygen Concentration (ppm)	Test Variables			Depth of Attack (mils)
	Temperature (°C)	Time (hr)	Pretest Heat Treatment	
150	816	100	Annealed 1 hr at 1000°C in vacuum	0
180	816	100	Annealed 1 hr at 1000°C in vacuum	0
190	816	100	Annealed 1 hr at 1000°C in vacuum	0
200	816	100	Annealed 1 hr at 1000°C in vacuum	0
250	816	100	Annealed 1 hr at 1000°C in vacuum	0
260	982	100	Annealed 1 hr at 1000°C in vacuum	0
290	816	100	Annealed 1 hr at 1000°C in vacuum	0
330	982	100	Annealed 1 hr at 1000°C in vacuum	0
410	816	24	Annealed 2 hr at 1800°C in vacuum	0
410	816	100	Annealed 2 hr at 1800°C in vacuum	0
450	982	100	Annealed 2 hr at 1300°C in vacuum	2
460	816	100	Annealed 2 hr at 1600°C in vacuum	1
500	816	100	Annealed 2 hr at 1600°C in vacuum	1
500	816	500	Annealed 2 hr at 1600°C in vacuum	1
500	982	100	Annealed 1 hr at 1000°C in vacuum	1.5

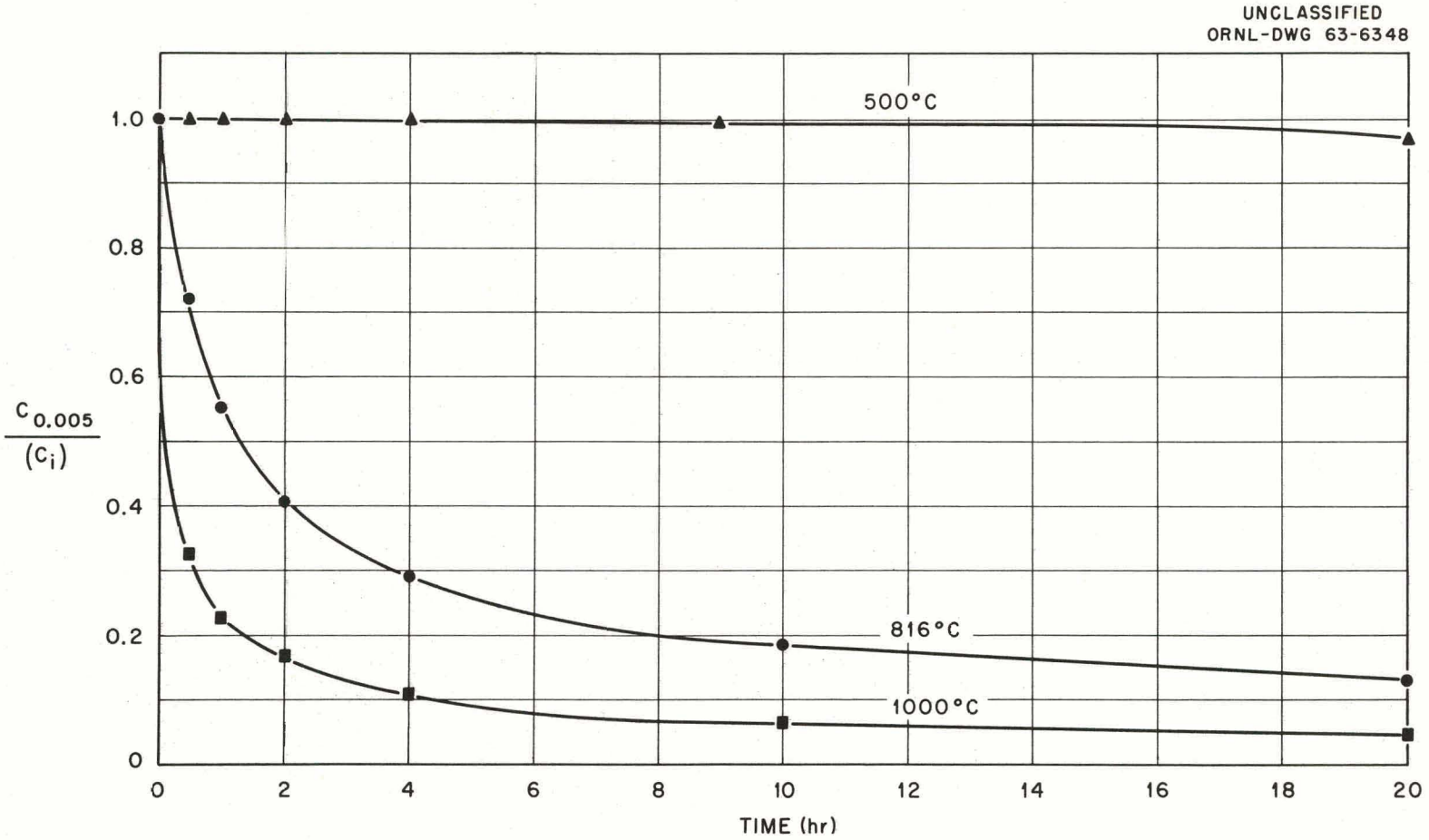

Figure 17. Ratio of oxygen concentration 0.005 inch from surface to initial oxygen concentration as a function of time.

surface to the initial concentration has been made as a function of time for the temperatures 500, 816, and 1000°C.* At 500°C the concentration would be unchanged from the initial value even after 20 hours exposure. However, the concentration can be reduced to half its initial value after approximately 75 minutes at 816°C and 5–10 minutes at 1000°C. Thus, for a starting concentration of 1000 parts per million oxygen, a point 0.005 inch from the surface would be reduced to 500 parts per million in 75 minutes at 816°C and in less than 10 minutes at 1000°C. If lithium penetration had not occurred at least to this depth prior to these times, then no further penetration would be expected since the oxygen concentration would be too low to support further penetration. Consequently, somewhat different results were obtained when polycrystalline specimens (Figure 18) and single-crystal specimens (Figure 19) were exposed to lithium at increasing temperatures. An increase in the depth of lithium penetration of polycrystalline samples occurred as the test temperature was increased from 260 to 1100°C. However, the single-crystal specimens exhibited less attack at 815 and 1040°C than at the two lower temperatures. This difference is believed to be related to the difference between the rate of lithium penetration and the rate of oxygen removal from the niobium. It was noted that the transgranular attack observed in the polycrystalline specimens tested at 260 and 540°C no longer occurred in the specimens

*See Appendix B for equations used to make these calculations.

UNCLASSIFIED
PHOTO 62268

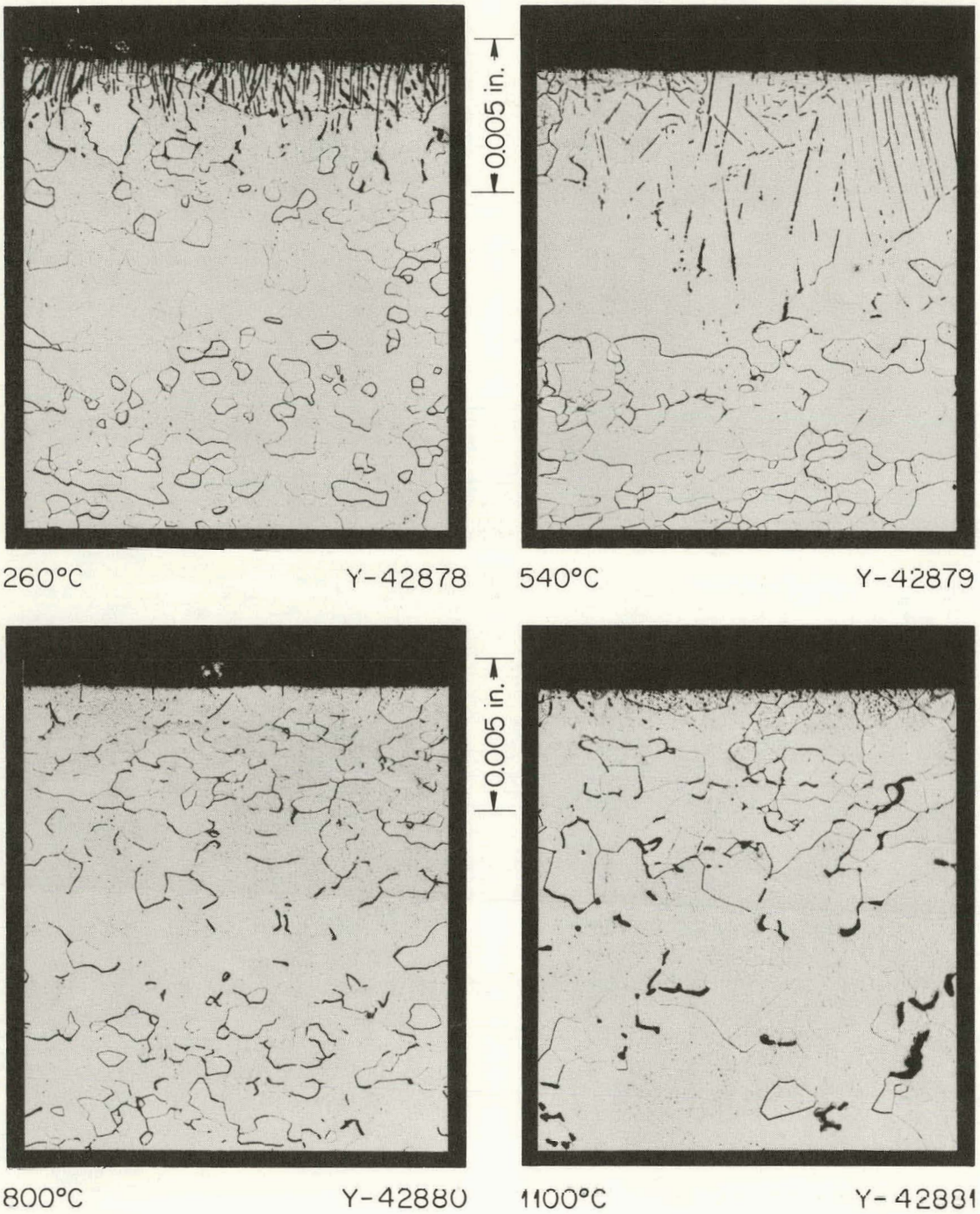

Figure 18. Effect of temperature on the depth of attack by lithium of polycrystalline niobium specimens containing 1000 parts per million oxygen. Test duration, 100 hours. Etchant: $HF-HNO_3-H_2SO_4-H_2O$.

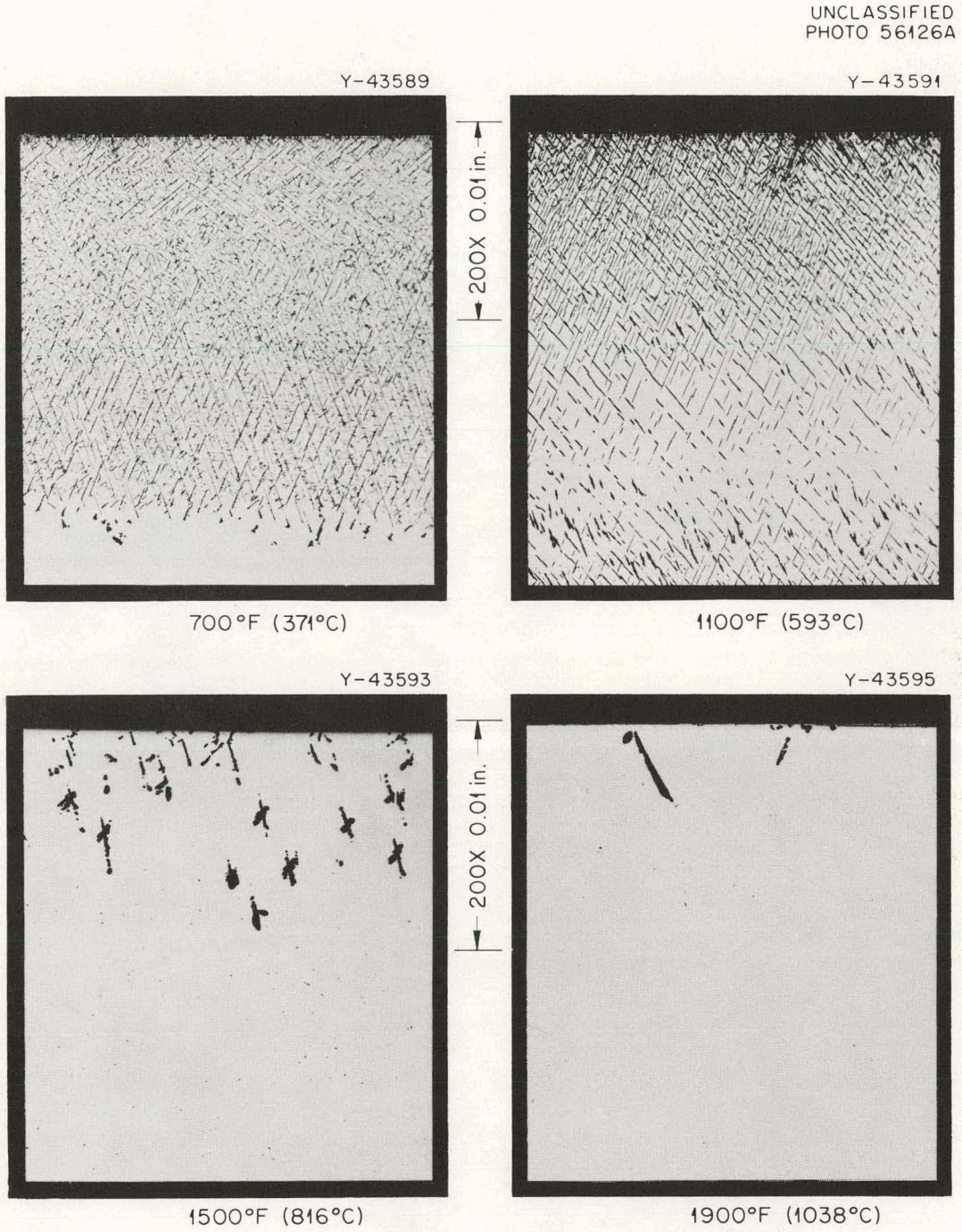

Figure 19. Effect of temperature on the depth of attack by lithium of a niobium single crystal containing 1500 parts per million oxygen. Test duration, 100 hours. Etchant: $HF-HNO_3-H_2SO_4-H_2O$. Reduced 17%.

tested at 800 and 1100°C. Corrosion of single-crystal specimens was necessarily restricted to the transgranular type of attack at all temperatures. It is postulated, therefore, that at high temperatures oxygen concentrations in the single-crystal specimens were rapidly reduced to levels too low to support further lithium penetration. On the other hand, penetration of the polycrystalline samples occurred entirely along grain boundaries at 800 and 1100°C, which indicated that the rate of grain-boundary penetration was more rapid than the oxygen removal rate from these areas. Since grain-boundary diffusion rates are generally more rapid than bulk diffusion rates, it appears that it was the faster rate of penetration by lithium along grain boundaries that was responsible for this effect.

Effect of Time

The effect of time on the rate and depth of attack was the next variable to be investigated. It was found that the rate of lithium penetration of niobium is initially very rapid — reaction product formation generally reached a maximum depth in less than 1 hour over a wide range of temperatures. An illustration of this effect is seen in Figure 20. The 0.040-inch-thick specimen in this figure was completely penetrated during a 0.5-hour exposure to lithium vapor at 1100°C. (The grain size and initial oxygen content [1900 parts per million] of this specimen were such that the oxygen level remained relatively high throughout the test.)

UNCLASSIFIED
PHOTO 59565

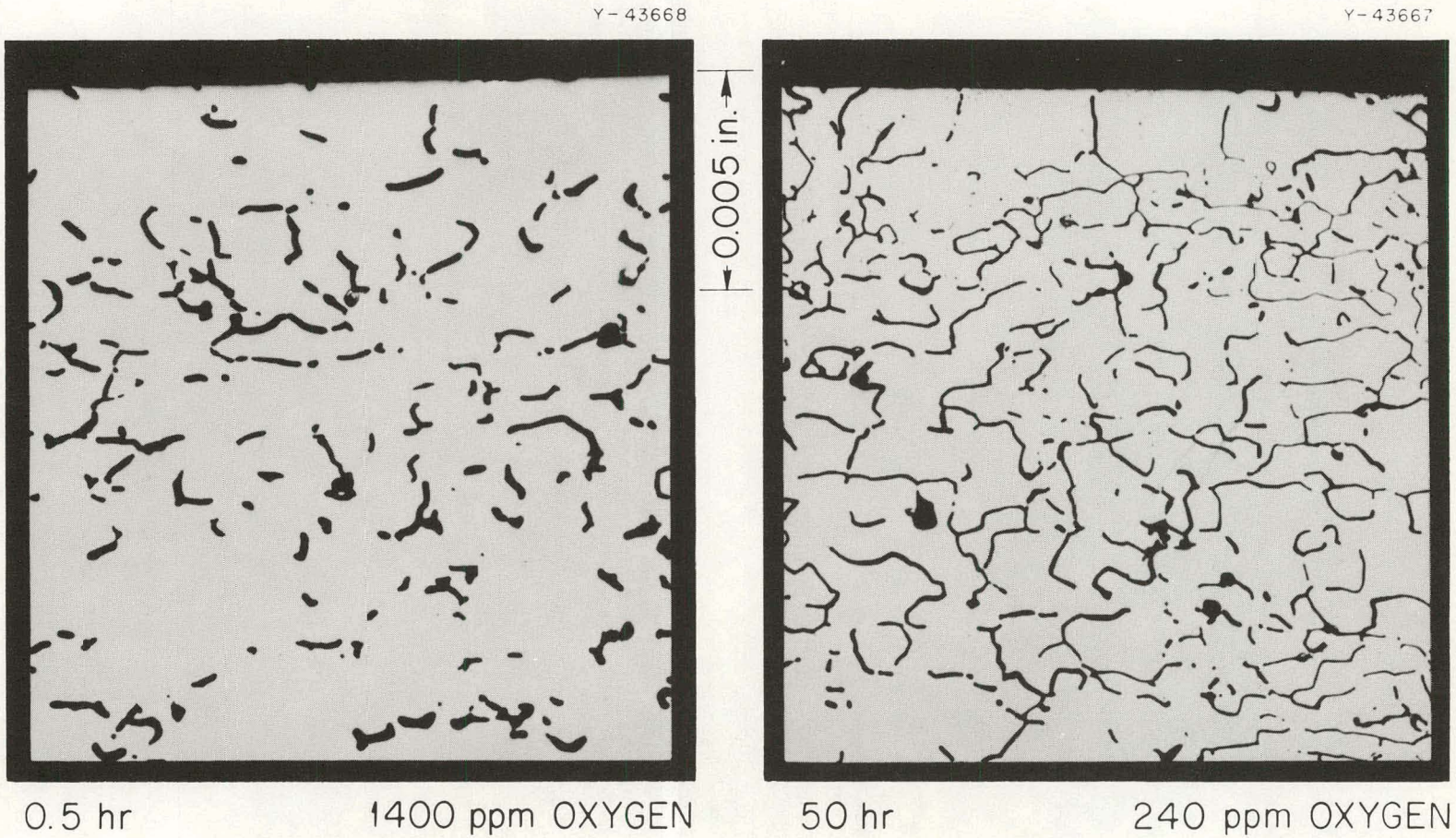

Figure 20. Effect of time on depth of attack by lithium vapor of polycrystalline niobium specimen containing 1900 parts per million oxygen. Test temperature, 1100°C. Posttest oxygen analysis showed oxygen decreased to 1400 parts per million after 0.5 hour and 240 parts per million after 50 hours. Etchant: $HF\text{-}HNO_3\text{-}H_2SO_4\text{-}H_2O$.

The depth of attack, as discussed in the previous section, is strongly affected by those variables which affect oxygen removal rate, such as grain size and initial oxygen concentration. In a series of tests in which exposure times were varied from 1 to 500 hours, no difference in depth of attack was observed at 816°C in niobium specimens initially containing 1000 parts per million oxygen. Typical results from this series are shown in Figure 21. Chemical analyses, however, showed that oxygen removal in these tests continued up to 100 hours. If the hardness profiles across these specimens are compared (Figure 22), a sharp gradient is evident in specimens tested for less than 100 hours. In each case, the first hardness measurement was made at a distance approximately 0.005 inch from the edge of the specimen. The hardness at this point for the specimen exposed for only 1 hour was less than 110 diamond pyramid hardness. From the plot of oxygen concentration versus hardness (Figure 7, page 22), it can be seen that this corresponds to an oxygen concentration of less than 500 parts per million – which is near the "threshold" concentration required for corrosion to occur. Therefore, depth of attack reached a maximum sometime within 1 hour, the exact time corresponding to the time when the oxygen content dropped below the critical level. Accordingly, the initial rate of attack was not measurable from the results of these tests.

Other tests in which depths of penetration were measured as a function of time are summarized in Table V. It can be seen that

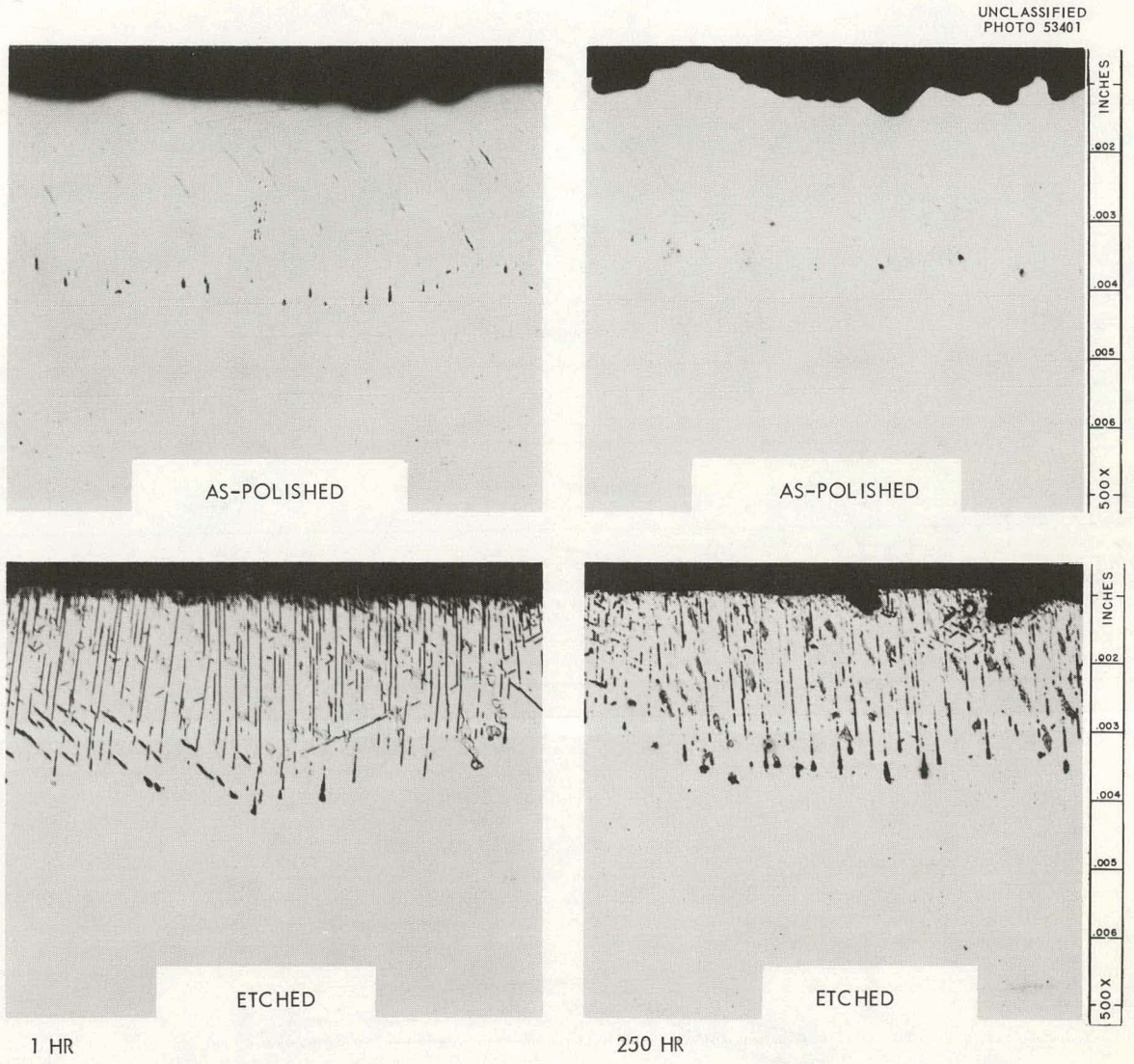

Figure 21. Effect of time on the depth of attack by lithium of niobium containing 1000 parts per million oxygen. Test temperature, 816 °C. Etchant: $HF-HNO_3-H_2SO_4-H_2O$. Reduced 27%.

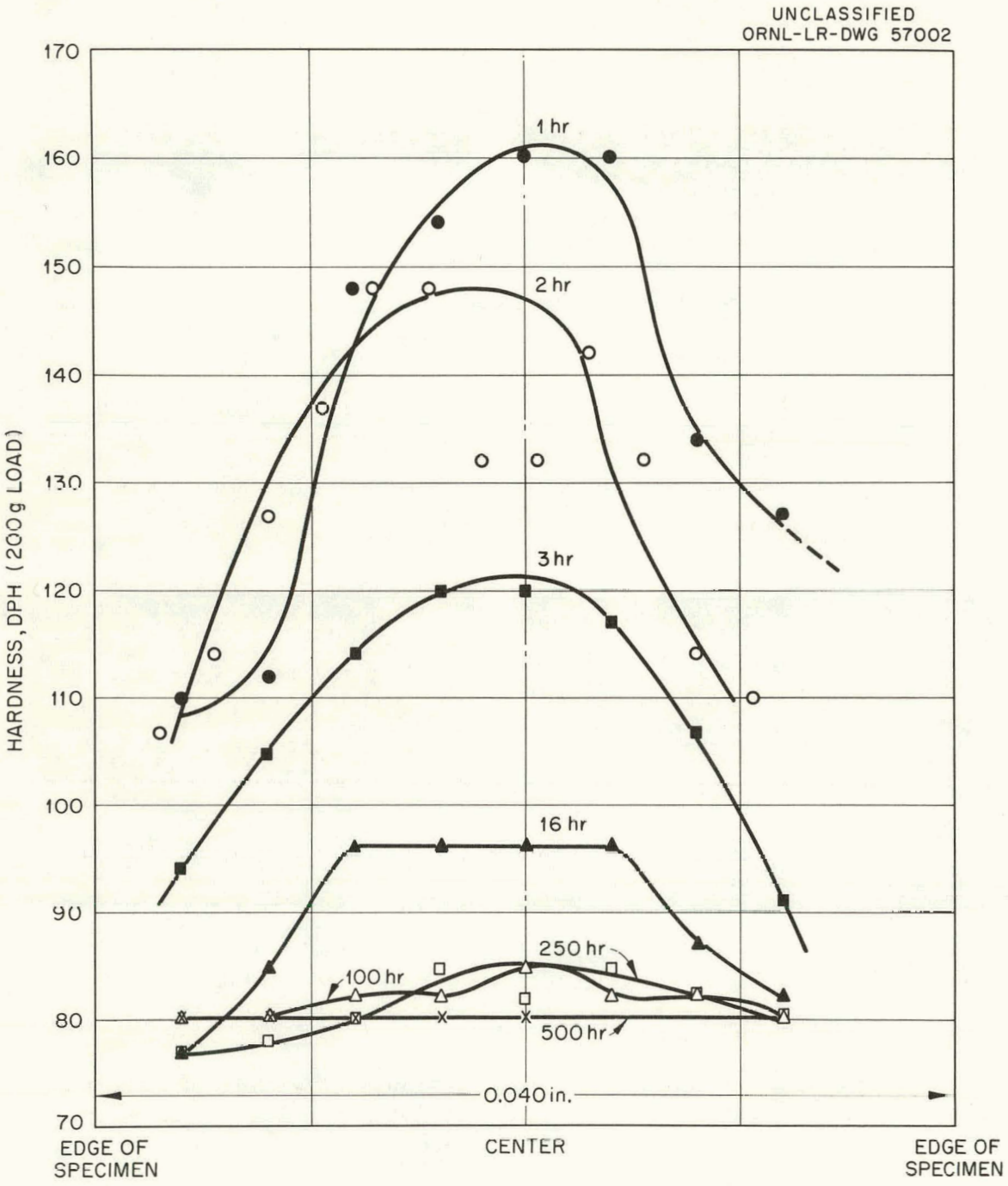

Figure 22. Hardness profile across niobium specimens following exposure to lithium for various times at 816°C.

TABLE V

EFFECT OF TIME ON THE DEPTH OF PENETRATION OF OXYGEN-CONTAMINATED NIOBIUM BY LITHIUM

Oxygen Concentration (ppm)	Type of Specimen	Temperature (°C)	Time (hr)	Depth of Attack (mils)
1000	Polycrystalline	260	1	7
1000	Polycrystalline	260	100	16
1000	Polycrystalline	538	1	9
1000	Polycrystalline	538	100	12
1700	Single crystal	816	0.1	3
1700	Single crystal	816	1	5
1700	Single crystal	816	100	30 (complete)
1700	Single crystal	816	1000	30 (complete)
1800	Single crystal	1093	0.5	0
1800	Single crystal	1093	50	13
1200	Single crystal	538	0.5	6
1200	Single crystal	538	30	13
4475	Single crystal	816	0.1	12
4475	Single crystal	816	1	33 (complete)
4475	Single crystal	816	100	33 (complete)

differences in depths of penetration of single-crystal specimens were observed only for times less than 1 hour. Thus, the point is made once again that the rate of lithium penetration is rapid, but the maximum depth of penetration which will occur depends on the rate at which oxygen is removed from the niobium. Since similar depths of penetration were observed at various temperatures, the corrosion process must be controlled by the rate at which lithium can reach the unattacked niobium and also by the requirement that the local oxygen concentration remain greater than approximately 400 parts per million.

Effect of Grain Size

Three different grain sizes were produced in niobium specimens by annealing for 1 hour at 1000, 1300, and 1600°C, respectively. Oxygen additions of 1300–1600 parts per million were then made at 1000°C, after which the specimens were exposed to lithium for 20 hours at both 400 and 1000°C. Results are shown in Figure 23. Although some grain-boundary attack occurred at both 400 and 1000°C for all grain sizes, it is apparent that grain-boundary attack is favored by small grain size and high temperatures. At 400°C depth of penetration increased with increasing grain size. This could have resulted because the path length that the lithium has to travel to reach a specific depth generally decreases with increasing grain size. The total volume of corrosion product could be the same in each case. For each grain size, the depth of penetration was greater at 1000 than at 400°C. Therefore, it must be concluded that the rate of grain-boundary

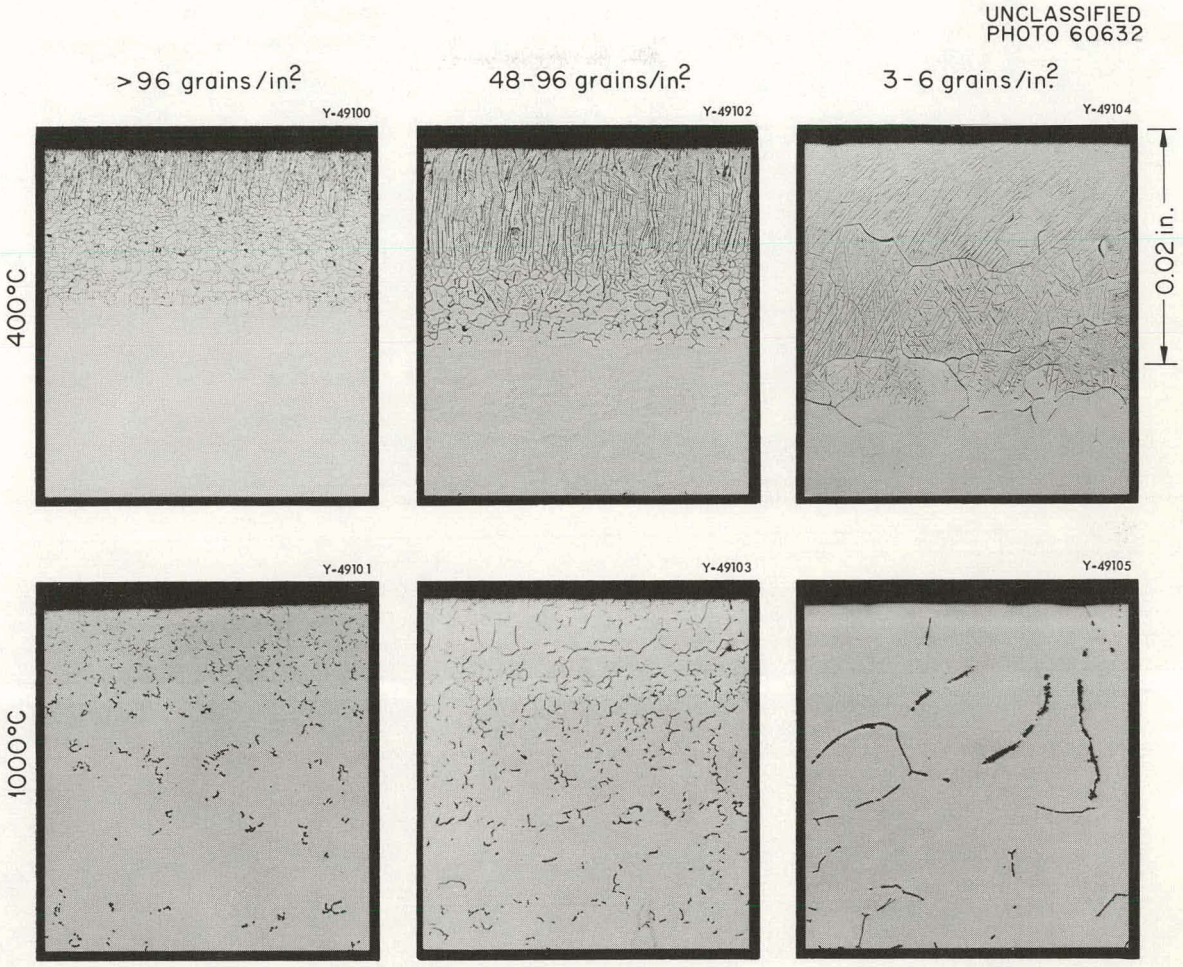

Figure 23. Effect of grain size and temperature on corrosion of niobium by lithium. Test duration, 20 hours. Etchant: $HF-HNO_3-H_2SO_4-H_2O$.

penetration increases with increasing temperature. In fact, the difference in rate of attack was even greater than suggested in Figure 23, page 53, since no change in the oxygen concentration of the three specimens tested at 400°C was found, while the three tested at 1000°C were all reduced to approximately 250 parts per million. Grain-boundary penetration must have occurred prior to the oxygen concentration being reduced to a value too low to support further penetration. The rate of transcrystalline penetration was apparently slower than the rate of grain-boundary penetration since the transcrystalline corrosion front was observed to lag the intergranular corrosion front at 400°C and was not observed at all at 1000°C.

Effect of Heat Treatment

Heat treating at different temperatures should produce different oxygen distributions in niobium which might be expected to affect the corrosion process. However, it was found that if other test variables such as oxygen concentration, temperature, and grain size were kept constant, then heat treating for 100 hours at 400, 600, or 800°C did not significantly alter the depth and pattern of corrosion. This indicates that differences in depth or type of attack are determined more by the local oxygen concentration at the corrosion interface rather than the original oxygen distribution.

Effect of Deformation

To determine if the amount of prior deformation affects the corrosion process, a single crystal was annealed at 1800°C to reduce

the number of dislocations, and a second single crystal having the same orientation was cold worked to increase the number of dislocations. Typical results from a number of such tests are presented in Figure 24 which shows two specimens treated as described above and then exposed to lithium for 1 hour at 500°C. No significant difference in depth of attack was noted.

Effect of Lithium Purity

Samples of pure niobium were not attacked when exposed to lithium plus 1 per cent Li_2O and lithium plus 1 per cent Li_3N for 100 hours at 816°C. In addition, single crystals of niobium containing 1000 parts per million oxygen were tested in lithium, lithium plus 0.5 per cent Li_2O, and lithium plus 0.5 per cent Li_3N, and complete attack was observed in all specimens. Therefore, it was concluded that oxygen and nitrogen in lithium do not contribute to penetration of niobium.

II. NIOBIUM ALLOYS

The addition of an alloying element was considered as one possible solution to this corrosion problem and was investigated by determining the effect of oxygen additions to niobium-zirconium and niobium-vanadium alloys on their corrosion resistance to lithium. It was suspected that zirconium, which forms a more stable oxide than those of niobium, should be effective in altering the oxygen stability in the alloy and thereby have an effect on its corrosion behavior.

UNCLASSIFIED
PHOTO 60631

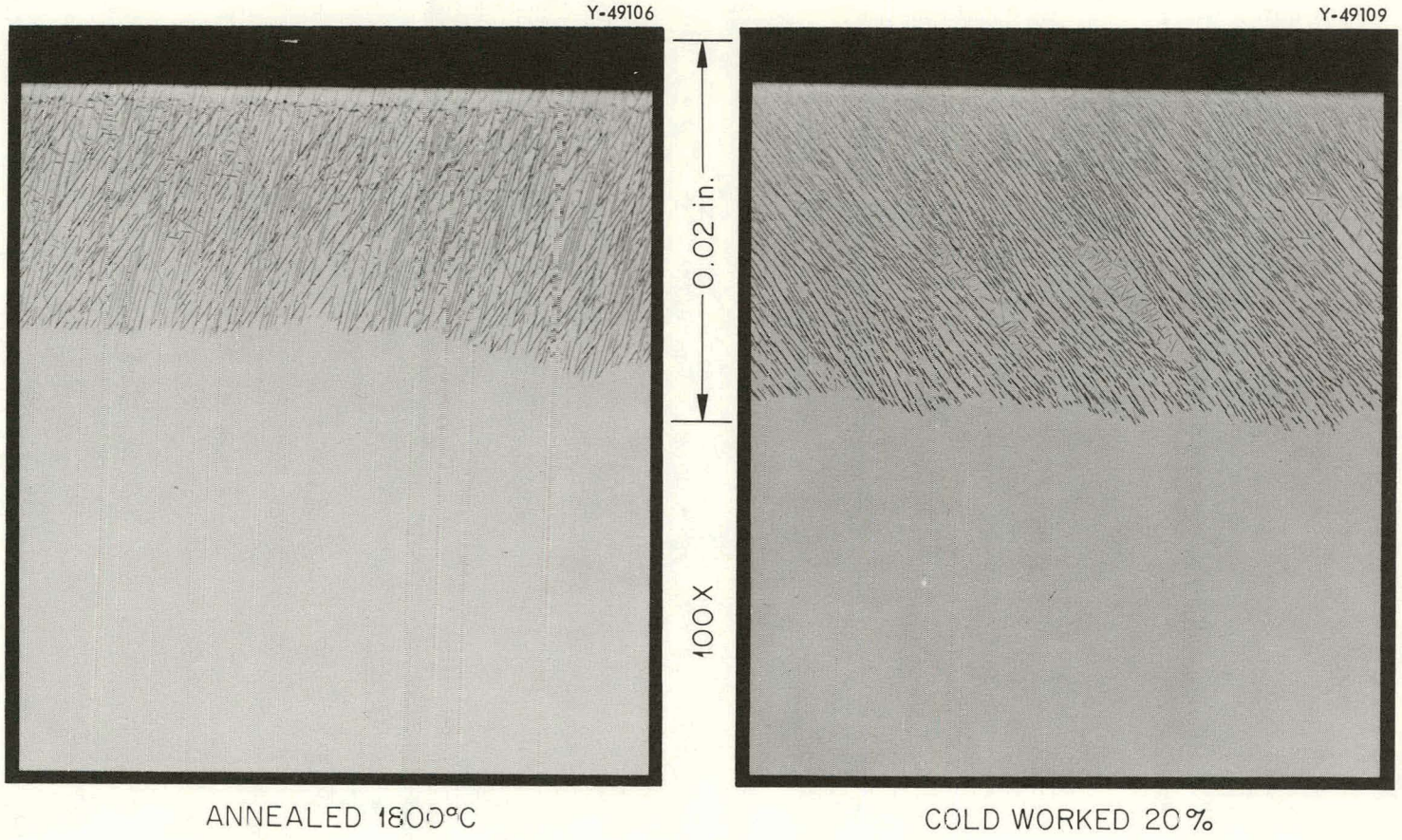

Figure 24. Effect of deformation on corrosion by lithium of a niobium single crystal containing 1700 parts per million oxygen. Test conditions, 1 hour at 500°C. Etchant: $HF-HNO_3-H_2SO_4-H_2O$.

Vanadium, on the other hand, forms oxides of approximately the same thermodynamic stability as niobium and therefore should be relatively ineffective.

Niobium-Zirconium Alloys

Systematic additions of oxygen to a niobium–1 per cent zirconium alloy were made at 1000 °C and subsequent exposure to lithium for 100 hours at 816 °C resulted in attack of the alloy in a manner similar to unalloyed niobium (Figure 25). Further studies revealed, however, that if the niobium–1 per cent zirconium was heat treated at 1300 °C after oxidation no lithium penetration occurred when specimens were tested as described above. These results were confirmed by a more detailed investigation in which both zirconium concentration and oxygen concentration were varied. Results from this test are summarized in Table VI. It can be seen that the corrosion protection obtained by heat treating at 1300 °C was a function of both zirconium and oxygen concentrations. When the oxygen-to-zirconium atomic ratio exceeded 2/1, no corrosion protection resulted even after heat treatment. Subsequent tests showed that other heat treatments such as 1 hour at 1600 °C or 5 hours at 1000 °C were also effective in producing a stable oxygen distribution in niobium–1 per cent zirconium (that is, a specimen which is not attacked by lithium), but only if the oxygen-to-zirconium atomic ratio did not exceed 2/1. Since this ratio corresponds to the stoichiometry of ZrO_2, it is postulated that corrosion protection results from the formation of this oxide in niobium-zirconium alloys. Mechanical relaxation measurements have been used by Stephenson and McCoy (22)

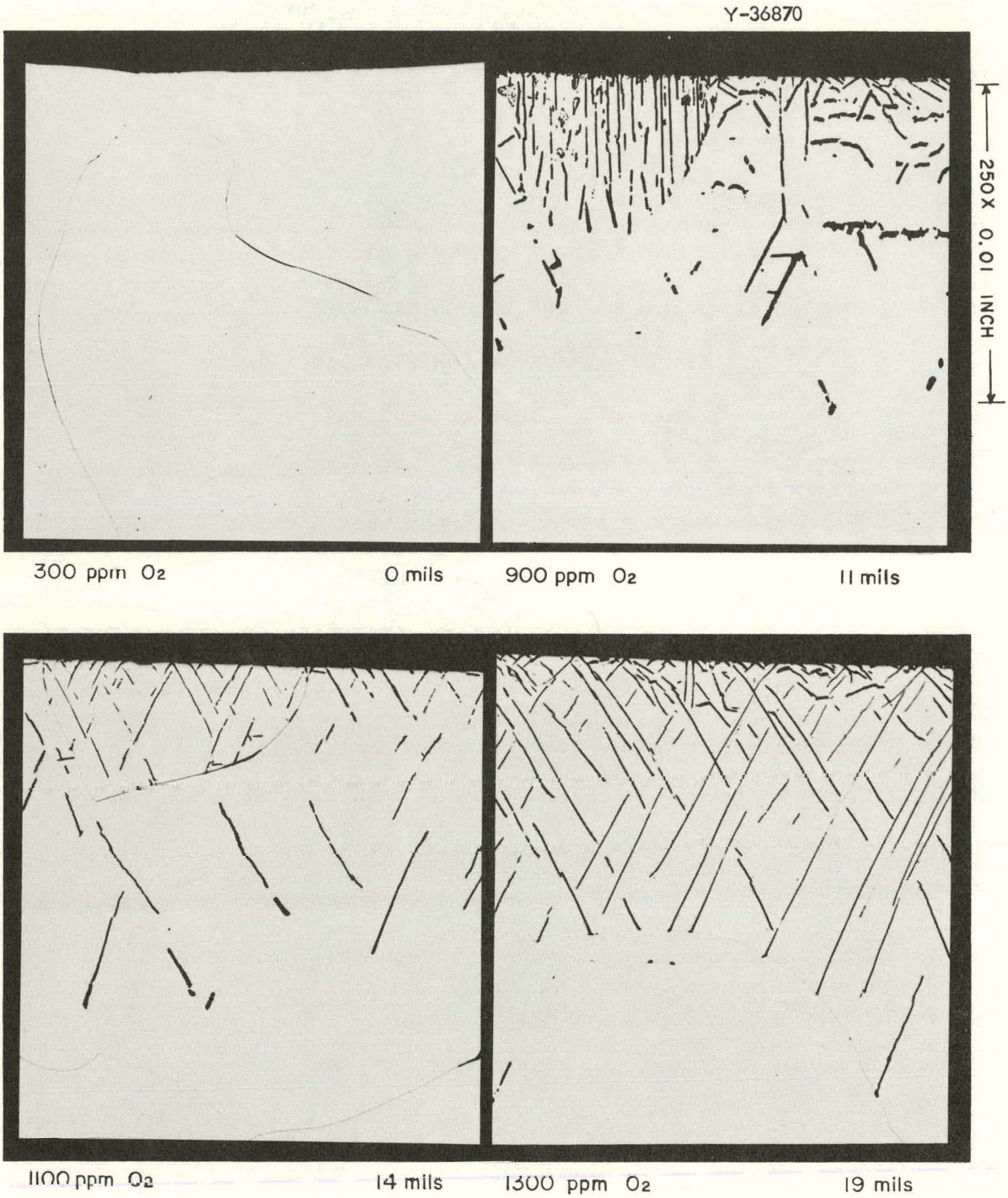

Figure 25. Effect of initial oxygen concentration, 300–1300 parts per million, in niobium–1 per cent zirconium alloy on depth of attack by lithium. Test conditions, 100 hours at 816°C. Etchant: $HF-HNO_3-H_2SO_4-H_2O$. Reduced 20%.

TABLE VI

DEPTH OF ATTACK BY LITHIUM OF NIOBIUM-ZIRCONIUM ALLOYS AS A FUNCTION OF ZIRCONIUM CONCENTRATION, OXYGEN CONCENTRATION, AND HEAT TREATMENT

Test Conditions: 100 hr at 816°C

Zirconium Concentration (%)	Oxygen Concentration (%)	Depth of Attack (mils)	
		After Oxidation at 1000°C*	After Heat Treatment at 1300°C**
0.05	0.09	15	15†
0.05	0.18	25	25†
0.05	0.23	30‡	30†
0.4	0.09	15	0
0.4	0.18	20	15†
0.4	0.23	30‡	30†
0.6	0.09	10	0
0.6	0.18	20	0
0.6	0.23	30‡	25†
0.9	0.09	10	0
0.9	0.18	20	0
0.9	0.23	30‡	0
1.3	0.09	5	0
1.3	0.18	10	0
1.3	0.23	25	0

*Specimen exposed to lithium after oxidation at 1000°C.

**Specimen heat treated in vacuum for 2 hours at 1300°C following oxidation and prior to exposure to lithium.

†Oxygen-to-zirconium atomic ratio was greater than 2.

‡Complete penetration of 60-mil-thick specimen.

to study the precipitation of interstitial solutes such as oxygen and nitrogen from supersaturated solid solution in niobium-zirconium alloys. (A discussion of the theory and mathematics upon which such measurements are based is beyond the scope of this paper, but has been presented elsewhere [23,24].) From these mechanical relaxation measurements, an internal friction spectrum of a niobium–0.16 per cent zirconium specimen containing 1070 parts per million oxygen was obtained (Figure 26). It was concluded that the peak which occurred at 220°C was caused by the stress-induced motion of oxygen atoms in the vicinity of a zirconium atom. This peak has been labeled "oxygen-zirconium interaction" to distinguish it from the normal niobium-oxygen and niobium-nitrogen peaks which also occurred. When 1500 parts per million oxygen was added to a niobium–1 per cent zirconium wire specimen at 1000°C, a similar "oxygen-zirconium interaction" peak was found. After annealing for 1 hour at 1000°C, the peak was almost completely suppressed indicating that the oxygen had precipitated from solution. These specimens were then tested in lithium for 20 hours at 500°C and the results are shown in Figure 27. Lithium penetration occurred in the specimen which had exhibited a zirconium-oxygen interaction peak; however, no penetration was observed in the specimen annealed at 1000°C. Evidence that the oxide phase which forms as a result of heat treating is ZrO_2 has been given by Hobson (25) who identified ZrO_2 as a precipitate in aged niobium–1 per cent zirconium alloys.

Heat treatments at temperatures from 1000 to 1600°C all proved effective in stabilizing the oxygen in niobium–1 per cent zirconium

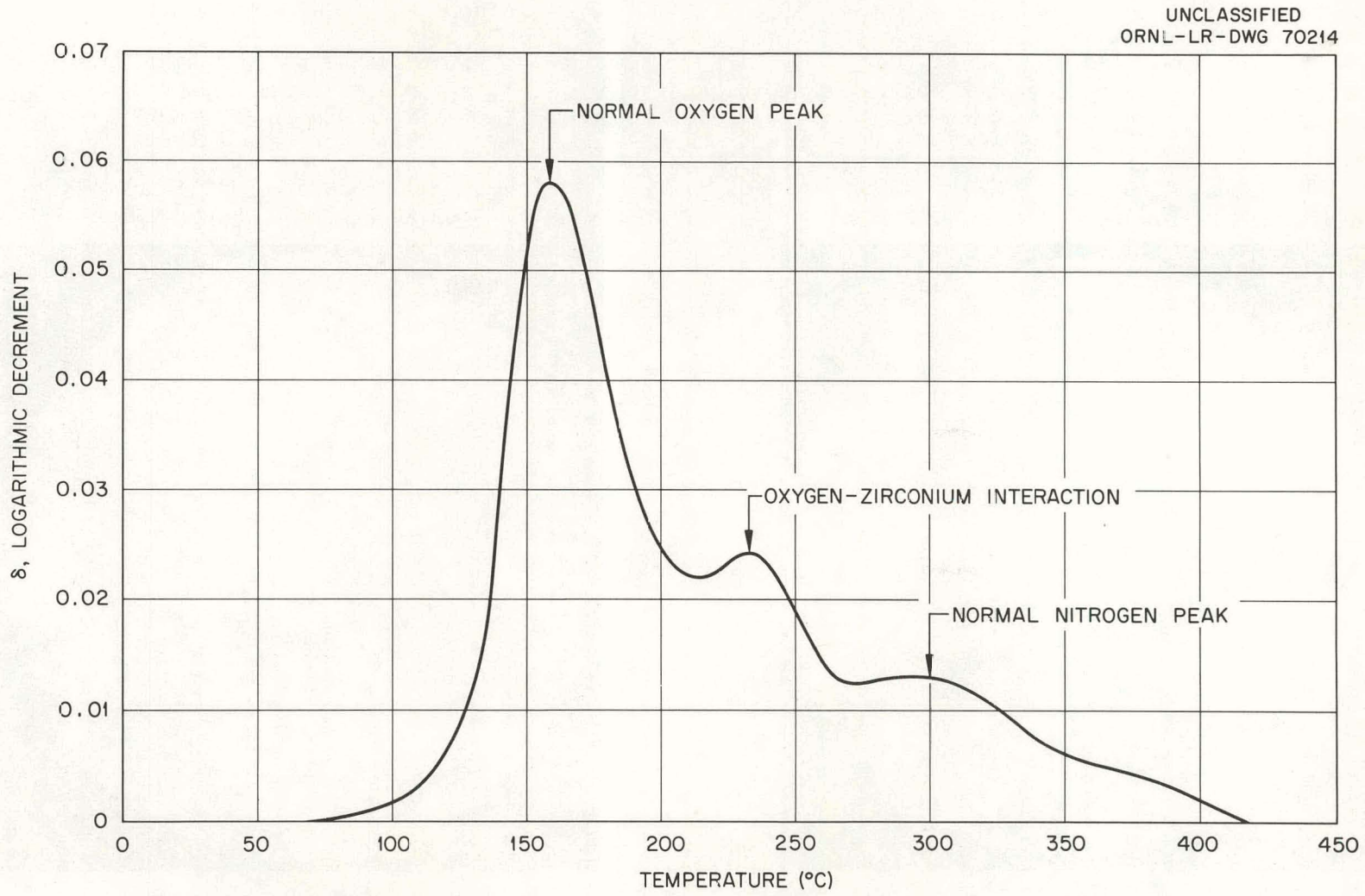

Figure 26. Internal friction spectrum of niobium–0.16 per cent zirconium alloy annealed at 1925°C.

UNCLASSIFIED
PHOTO 63385

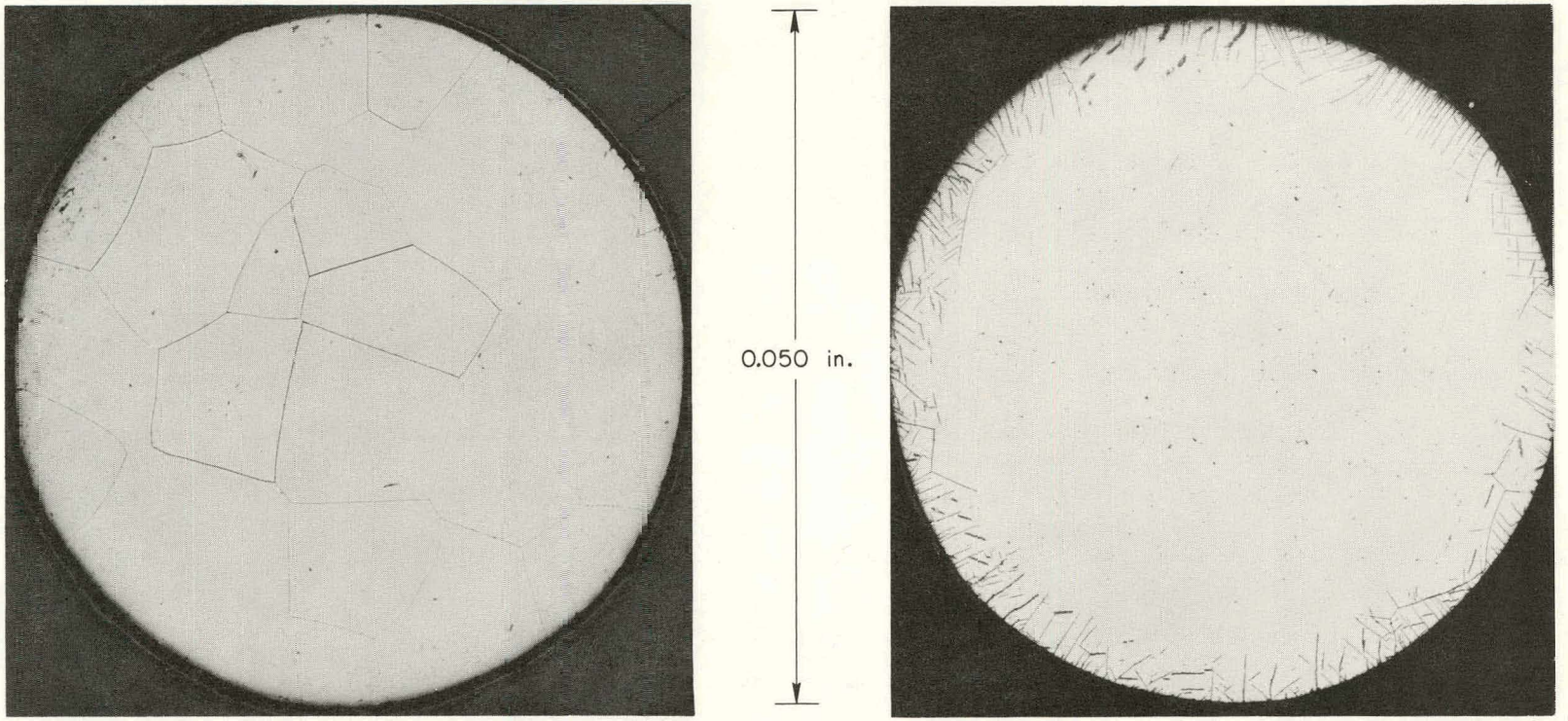

(a) SPECIMEN HAVING NO Zr-O INTERACTION PEAK.
INITIAL OXYGEN CONCENTRATION: 1500 ppm

(b) SPECIMEN HAVING Zr-O INTERACTION PEAK.
INITIAL OXYGEN CONCENTRATION: 1500 ppm

Figure 27. Niobium-1 per cent zirconium alloy following exposure to lithium for 1 hour at 500°C. Both specimens were oxidized at 1000°C, but specimen (a) was annealed for 1 hour in vacuum following oxidation while specimen (b) was not.

alloys. However, when the annealing temperature was raised to 2000°C, a specimen to which 900 parts per million oxygen had been added was completely attacked upon exposure to lithium for 100 hours at 800°C. Also, niobium–1 per cent zirconium specimens which were welded after oxygen additions did not exhibit corrosion resistance. When heated by annealing or welding into the range where ZrO_2 redissolves, the oxygen is then in solid solution in an unstable form which renders the alloy susceptible to lithium attack.

The effect of lithium penetration on the mechanical properties of niobium–1 per cent zirconium is shown in Table VII. Specimens were made from 0.040-inch sheet and were the same size as reported earlier for unalloyed niobium. Oxygen was added at 1000°C, and specimens were tensile tested after the following treatments:

1. Oxidation.
2. Oxidation followed by testing in lithium 100 hours at 816°C.
3. Oxidation followed by heat treating in vacuum for 1 hour at 1600°C.
4. Oxidation followed by heat treating in vacuum for 1 hour at 1600°C and then testing in lithium for 100 hours at 816°C.
5. Oxidation followed by heat treating in vacuum for 1 hour at 1600°C and then heat treating in argon for 100 hours at 816°C.

The addition of oxygen at 1000°C resulted in a large increase in tensile strength but decreased the per cent elongation to zero. After exposure to lithium these specimens showed a decrease in tensile strength, and their ductility also remained low. This decrease in strength and low ductility is similar to the results found with unalloyed niobium. If heat treated at 1600°C following oxidation, both

TABLE VII

EFFECT OF OXYGEN IN NIOBIUM–1 PER CENT ZIRCONIUM ALLOY ON ITS ROOM-TEMPERATURE TENSILE PROPERTIES BEFORE AND AFTER EXPOSURE TO LITHIUM

Oxygen Concentration (ppm)	Treatment*	Tensile Strength (psi)	0.2% Offset Yield Strength (psi)	Elongation in 2 Inches (%)
150	a	53,700	46,700	11.0
310	a	64,400	57,800	11.0
650	a	97,300	97,300	2.0
1200	a	125,200	125,200	0.0
2100	a	137,700	137,700	0.0
3260	a	119,900	119,900	0.0
340	b	63,700	58,800	6.0
940	b	62,700	60,000	2.5
1370	b	46,800	46,800	1.0
1630	b	43,800	43,800	0.5
100	c	38,700	35,600	14.0
290	c	37,300	33,300	10.0
560	c	38,800	33,200	11.0
860	c	35,700	33,100	11.0
1360	c	35,800	28,600	14.0
100	d	32,500	28,700	13.5
430	d	32,700	28,800	8.5
480	d	32,300	28,400	11.5
1130	d	33,100	26,700	10.5
1430	d	32,000	24,100	13.5
100	e	35,600	32,100	11.0
440	e	33,500	29,800	9.5
480	e	32,400	28,400	10.5
1140	e	35,800	29,300	12.0
1390	e	32,700	27,200	12.0

*a. Oxidation.

b. Oxidation followed by testing in lithium 100 hours at 816 °C.

c. Oxidation followed by heat treating in vacuum for 1 hour at 1600 °C.

d. Oxidation followed by heat treating in vacuum for 1 hour at 1600 °C and then testing in lithium for 100 hours at 816 °C.

e. Oxidation followed by heat treating in vacuum for 1 hour at 1600 °C and then heat treating in argon for 100 hours at 816 °C.

tensile strength and elongation remained constant with increasing oxygen and were decreased only slightly after further treatment in lithium or argon at 816°C. If the stable condition reached after a 1600°C heat treatment is the result of the formation of ZrO_2 in the alloy, it would appear that, when precipitated under these conditions, the loss in strength which should result when zirconium is precipitated from substitutional solid solution is just offset by the strengthening which occurs upon precipitation of ZrO_2.

Niobium-Vanadium Alloys

The addition of 40 per cent vanadium to niobium did not prove effective in altering the corrosion resistance of the niobium to lithium even after heat treatment at 1300°C. As shown in Figure 28, after the addition of 1000 parts per million oxygen to a niobium–40 per cent vanadium alloy, considerable grain-boundary attack resulted during exposure to lithium for 100 hours at 816°C. Therefore, either the oxygen is not preferentially associated with vanadium, or if it is associated with the vanadium, it is in a form that is susceptible to attack by lithium.

III. OTHER REFRACTORY METALS

Results of tests with tantalum at 816°C were similar to those obtained on niobium. Tantalum, however, was more sensitive to oxygen concentration than niobium. As shown in Figure 29, complete penetration of a 0.040-inch specimen occurred with an initial oxygen

UNCLASSIFIED
PHOTO 56329

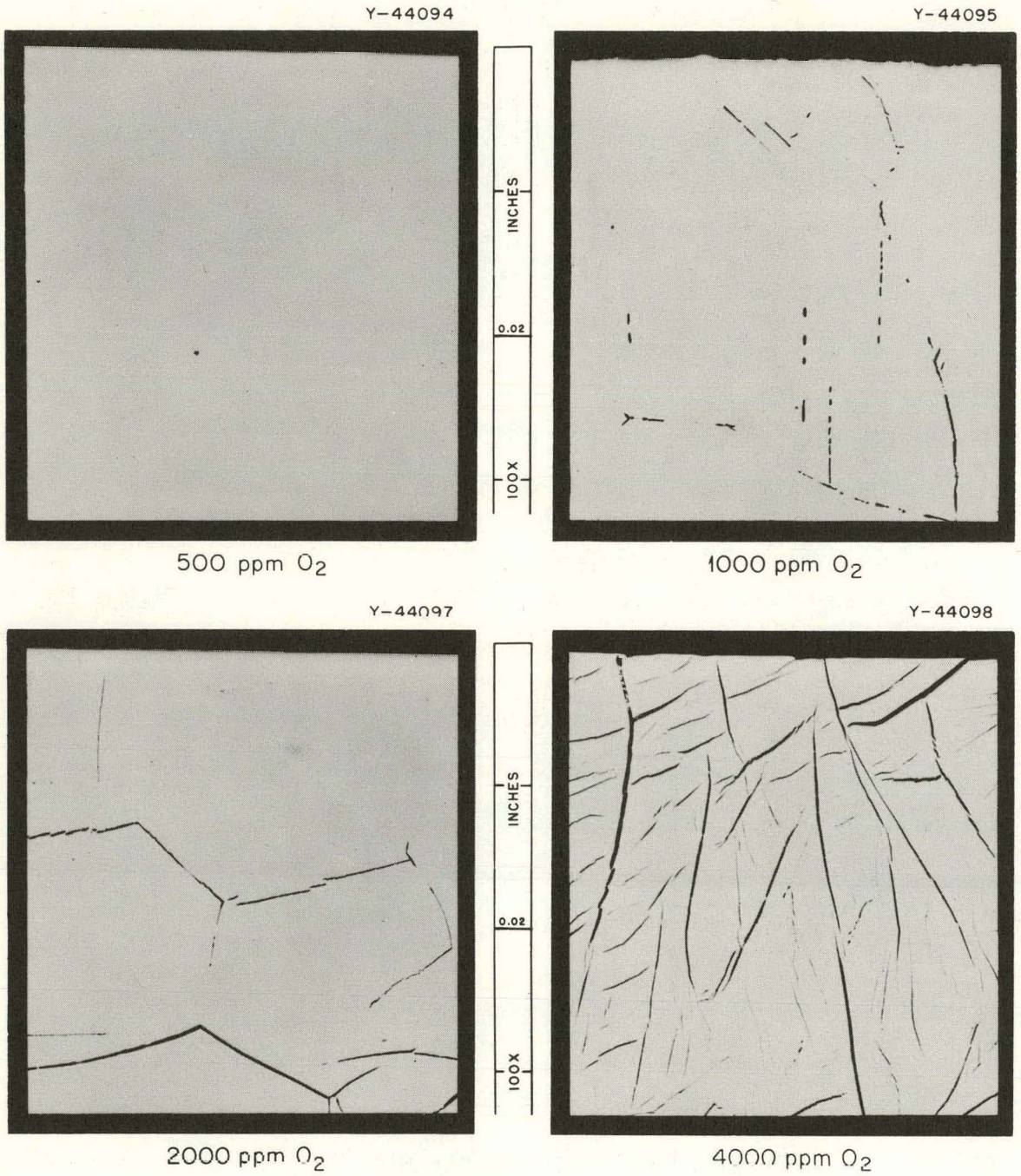

Figure 28. Effect of oxygen concentration of niobium–40 per cent vanadium alloy on its corrosion resistance to lithium. Test conditions, 100 hours at 816°C. As-polished. Reduced 14%.

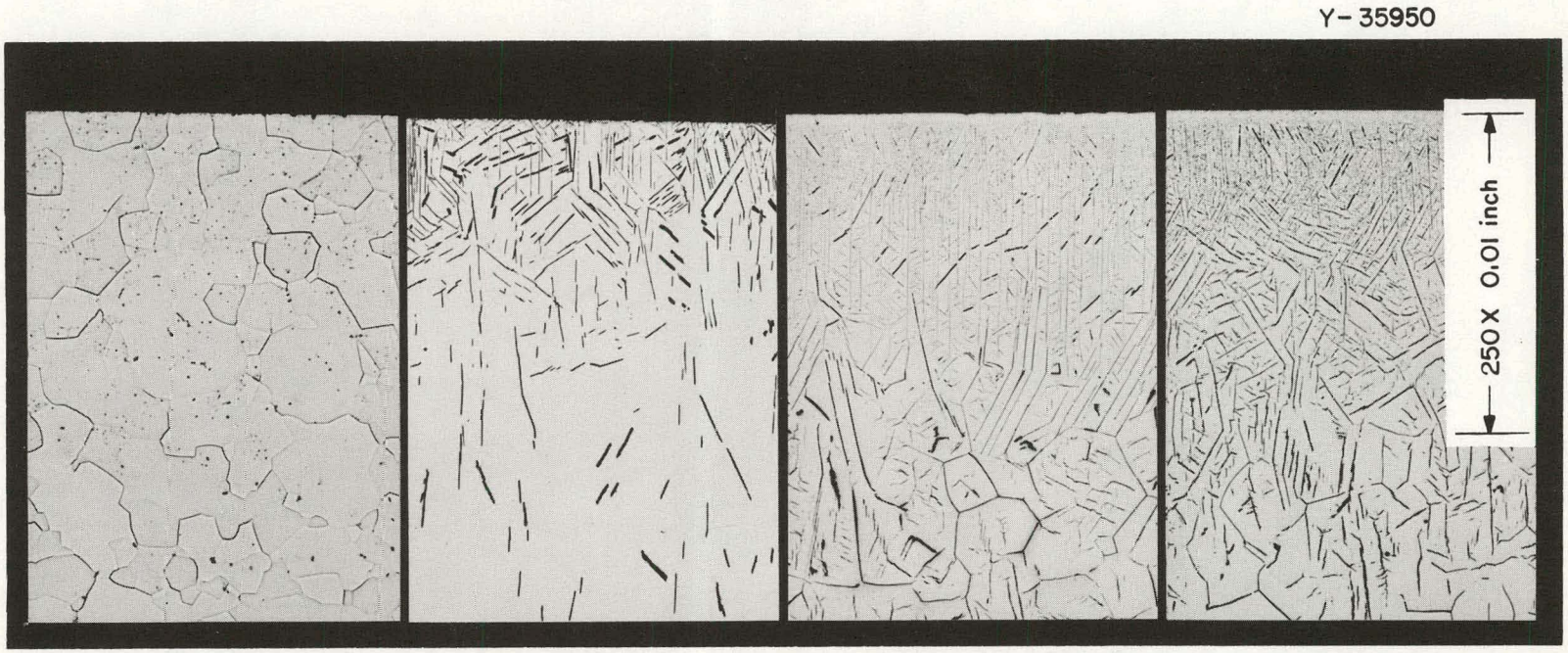

Figure 29. Effect of initial oxygen concentration in tantalum on its corrosion resistance to lithium. Test conditions, 100 hours at 816°C. Etchant: $HF-HNO_3-H_2SO_4-H_2O$. Reduced 36%.

concentration of 300 parts per million. This indicates the threshold concentration for corrosion of tantalum is considerably less than for niobium. Posttest chemical analyses indicated that oxygen had been gettered from the tantalum by lithium.

The effect of oxygen in zirconium, titanium, and vanadium was also investigated. Oxygen in these metals did not affect their corrosion resistance. Additions of 2000 parts per million oxygen were made to vanadium and 4000 parts per million to titanium and zirconium, but no evidence of lithium penetration was detected after 100-hour exposures at 816°C. It is interesting to note that although zirconium additions to niobium were effective in producing a corrosion resistant alloy and vanadium additions were not, both were individually unaffected by the presence of oxygen. This supports the theory that oxygen in niobium-zirconium alloys is associated with the zirconium, but that it is not preferentially associated with vanadium in niobium-vanadium alloys.

Although no lithium penetration of zirconium, titanium, or vanadium was found, oxygen redistribution did occur. These results, along with those for tantalum and niobium, are given in Table VIII. Niobium, tantalum, and vanadium all lost oxygen to the lithium even at initial concentrations as low as 150 parts per million, but titanium and zirconium gettered oxygen from the lithium when their initial oxygen concentrations were less than approximately 1000 parts per million. It would be of interest to know the equilibrium distribution of oxygen between these metals and lithium at various temperatures.

TABLE VIII

OXYGEN CONCENTRATION IN REFRACTORY METALS BEFORE AND AFTER EXPOSURE TO LITHIUM FOR 100 HOURS AT 816 °C

Material	Oxygen Concentration (ppm) Before Test	After Test
Niobium	150	90 (50)*
	500	210 (60)
	650	370 (150)
	1000	460 (290)
	1700	660 (350)
Tantalum	220	80
	450	100
	1100	150
	2000	250
Vanadium	400	80
	800	110
	2200	180
Titanium	120	560
	600	670
	1100	930
Zirconium	740	800
	1000	810
	1600	1000

*Analyses in parentheses are on same specimen after it was machined to remove the corrosion product.

However, since the niobium-oxygen-lithium and tantalum-oxygen-lithium systems are complicated by the formation of a corrosion product containing oxygen and since direct analysis of lithium for oxygen is difficult, no measurements of this type were attempted.

APPENDIX A

DERIVATION OF EXPRESSION TO CALCULATE DISTRIBUTION COEFFICIENT FOR OXYGEN* IN REFRACTORY METAL–LIQUID METAL SYSTEMS

Consider two immiscible solvents A and B in contact, both containing oxygen in solution. Then

$$\bar{F}_A = F_A^\circ + RT \ln a_A , \tag{1}$$

where $\bar{F}_A$ is the partial free energy of oxygen per gram atom in A, F_A° is the free energy per gram atom of oxygen in a reference state, and a_A is the activity of oxygen in A. Similarly, in solvent B the partial free energy of oxygen per gram atom can be written as

$$\bar{F}_B = F_B^\circ + RT \ln a_B . \tag{2}$$

Since at equilibrium $\bar{F}_A = \bar{F}_B$, it can be shown that

$$\ln \frac{a_B}{a_A} = \frac{F_A^\circ - F_B^\circ}{RT} . \tag{3}$$

A useful reference state for oxygen in this case is oxygen in solution in A or B which is in equilibrium with the oxides of A or B. For this choice of reference state F_A° can be replaced by $\Delta F^\circ_{f(\text{A oxide})}$ and F_B° by $\Delta F^\circ_{f(\text{B oxide})}$, where ΔF_f° refers to the standard free energy of formation of the oxides of A or B. Therefore

$$\frac{a_B}{a_A} = \exp\left[\frac{\Delta F^\circ_{f(\text{A oxide})} - \Delta F^\circ_{f(\text{B oxide})}}{RT}\right] . \tag{4}$$

---

*Similar derivation can be used also for other impurities which are in solution in both solid- and liquid-metal phases.

If the activity of oxygen in the dilute solutions involved can be expressed by an equation of the type

$$a_B = k_B N_B$$

where N_B is the atomic fraction of oxygen in B and k_B is a constant, then

$$a_B = \frac{N_B}{(N_B)_s} \quad ,$$

since $a_B = 1$ when $N_B = (N_B)_s$ (atomic fraction of oxygen soluble in B at temperature T), and similarly

$$a_A = \frac{N_A}{(N_A)_s} \quad .$$

At low concentrations

$$a_A = \frac{C_A}{(C_A)_s} \text{ and } a_B = \frac{C_B}{(C_B)_s} \quad ,$$

where C stands for concentration. Equation 4, page 72, can therefore be expressed as

$$\frac{C_B}{C_A} = \exp\left[\frac{\Delta F^o_{f(\text{A oxide})} - \Delta F^o_{f(\text{B oxide})}}{RT}\right] \frac{(C_B)_s}{(C_A)_s} \quad . \tag{5}$$

The right side of equation 5 is a constant at a given temperature and is called the distribution coefficient K_T ,

$$K_T = \frac{C_B}{C_A} \quad . \tag{6}$$

A comparison of experimentally measured values of the distribution coefficient with calculated values obtained from equation 5, page 73, (26,27) does not show good agreement. Some possible reasons for this discrepancy could be:

1. Errors in ΔF^{O}. High-temperature free energies of formation data are scarce and are usually the result of extrapolations from data near room temperature. Because ΔF^{O} is an exponential term in equation 5, page 73, small errors in ΔF^{O} can cause large errors in the calculated ratio. For example, errors of ±20 per cent in ΔF^{O} for Li_2O and NbO at 800°C could cause the calculated ratio to be in error by $10^{\pm 9}$. In addition, it is assumed that one knows the oxide species which is in equilibrium with the solution phase, since it is the ΔF_f^{O} of this specie which must be used in the calculation.

2. Solubilities Not Considered. In deriving equation 5, page 73, the assumption was made that A oxide dissolves only in metal A, and B oxide dissolves only in metal B. Other solubilities such as A in B, A oxide in B, B oxide in A were not considered.

3. Presence of Other Oxygen-Containing Species. Equation 5, page 73, describes a relation for only one oxygen-containing specie in each phase. If any additional oxygen-containing species are present in either phase, then, since methods of oxygen analysis usually measure the

total oxygen concentration present, no good correlation between calculated and experimental values would be expected.

4. Nonideality of Oxygen in Solution. It is assumed that the activity of oxygen in solution in either phase is a linear function of the oxygen concentration at saturation. If deviations from this relationship occur, the calculated values will be in error.

5. Experimental Errors. In determining the distribution coefficient, one must measure the oxygen concentration in both the solid and liquid metal at equilibrium. Analytical methods for analyzing oxygen in liquid metals are not very accurate. Indirect methods of analysis often require exposure of the liquid metal to contaminating atmospheres. In addition, the formation of surface films on some solid metals during the test leads to the conclusion that equilibrium may not always be attained.

APPENDIX B

DIFFUSION OF OXYGEN OUT OF NIOBIUM

Oxygen is gettered from niobium by lithium. The gettering reaction presumably occurs at the niobium surface, and the flow of oxygen toward the surface can be expressed by Fick's second law.

$$\frac{\partial C_{oxygen}}{\partial t} = D \frac{\partial^2 C_{oxygen}}{\partial x^2} \tag{7}$$

where

C_{oxygen} = concentration of oxygen,

D = diffusion coefficient, cm^2/sec,

x = distance from the surface, cm,

t = time, sec.

The boundary conditions for the gettering of oxygen by lithium are:

$C = C_o$ at $t = 0$, $0 < x \leq \ell$

$C = C_s$ at $x = 0$, $0 < t \leq \infty$

where

C_o = initial oxygen concentration in the niobium,

C_s = oxygen concentration at the surface,

ℓ = thickness of niobium specimen.

As shown in Figure 22, page 50, the concentration of dissolved oxygen near the surface is very rapidly reduced to a low level. If it is assumed that $C_s = 0$ for $t > 0$, then equation 7 has the following solution in terms of depth x and time t

$$C(x,t) = \frac{4C_o}{\pi} \sum_{n=o}^{\infty} \frac{1}{2n+1} \sin\left[\frac{(2n+1)\pi x}{\ell}\right] \exp\left[\frac{-D(2n+1)^2\pi^2 t}{\ell^2}\right] \quad (8)$$

where n is any integer from 0 to infinity and the other terms have their usual significance. Although equation 8 can be used to calculate C(x,t) for any values of D, ℓ, and t, it is useful to consider the semi-infinite condition which would hold if the concentration in the middle of the sample remains unchanged. This is shown schematically in Figure 30. In this case, a more useful solution to equation 7, page 76, is in terms of the error function which is

$$\frac{C}{C_o} = \text{erf}\ \frac{x}{2\sqrt{Dt}} \quad . \quad (9)$$

If one considers the situation where the concentration at the middle of the specimen has not decreased by more than 10 per cent (that is, $\frac{\ell}{\sqrt{Dt}} > 5$), then equation 9 affords an excellent approximation to equation 8.

Equations 8 and 9 were used to calculate $\frac{C}{C_o}$ at x = 0.005 inch as a function of time at 500 and 1000°C. Values of the diffusion coefficient for oxygen in niobium were obtained from the equation given by Ang (28):

$$D = 0.0147 \exp\left[\frac{-27,600}{RT}\right] \quad (10)$$

where

D = diffucion coefficient in cm^2/sec,

T = temperature in °K.

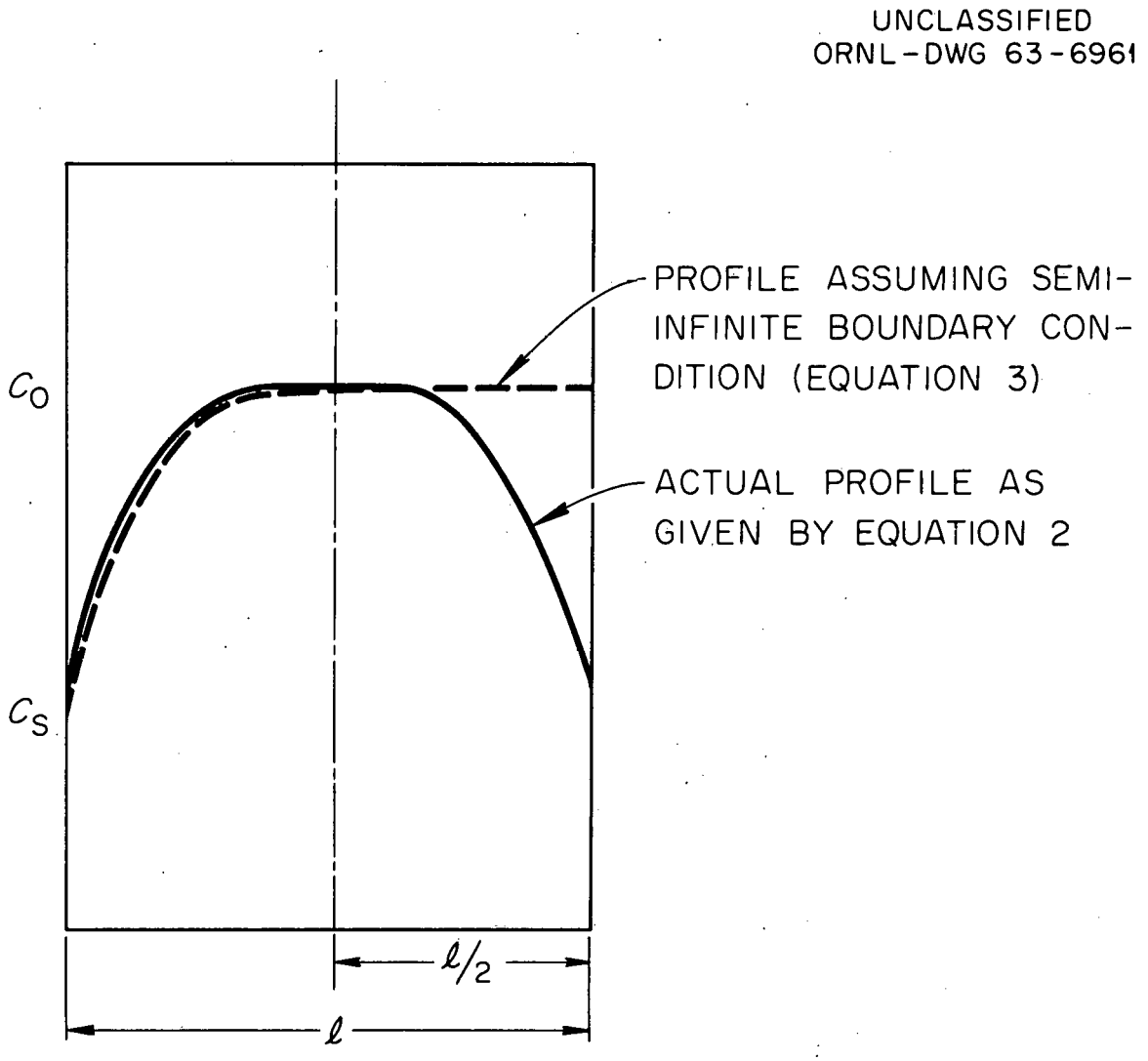

Figure 30. Concentration profile for oxygen diffusing out of niobium.

LIST OF REFERENCES

1. Brasunas, A. deS., Interim Report on Static Liquid Metal Corrosion, USAEC Report ORNL-1647 (May, 1954), pp. 32–44.

2. Jesseman, D. S., et al., Preliminary Investigations of Metallic Elements in Molten Lithium, USAEC Report NEPA-1465 (June, 1950).

3. Hoffman, E. E., Corrosion of Materials by Lithium at Elevated Temperatures, USAEC Report ORNL-2924 (October, 1960).

4. Kelman, L. R., W. D. Wilkinson, and F. L. Yagee, Resistance of Materials to Attack by Liquid Metals, USAEC Report ANL-4417 (July, 1950), pp. 7–9.

5. Miller, E. C., "Corrosion of Materials by Liquid Metals," Liquid Metals Handbook, NAVEXOS P-733 (Rev.), Atomic Energy Commission and Department of the Navy, 1952, pp. 144–45.

6. Brasunas, A. deS., "Liquid Metal Corrosion," Corrosion, 9, 78–84 (1953).

7. Manly, W. D., "Fundamentals of Liquid Metal Corrosion," Corrosion, 12(7), 46–52 (1956).

8. DiStefano, J. R., and E. E. Hoffman, Corrosion Mechanisms in Refractory Metal–Alkali Metal Systems, USAEC Report ORNL-3424 (August, 1963).

9. Bychkov, U. F., A. N. Rozanov, and V. B. Yakobleva, "The Solubility of Metal in Lithium," Atomnaya Energiya, 7(6), 531–36 (1959).

10. Hoffman, op. cit., ORNL-2924, p. 123.

11. Hoffman, E. E., Effects of Oxygen and Nitrogen on the Corrosion Resistance of Columbium to Lithium at Elevated Temperatures, USAEC Report ORNL-2675 (January, 1959).

12. Hoffman, E. E., "Solubility of Nitrogen and Oxygen in Lithium and Methods of Lithium Purification," Symposium on Newer Metals, Special Technical Publication No. 272, American Society for Testing Materials, Philadelphia, Pennsylvania, 1959, pp. 195–206.

13. White, J. C., et al., Aircraft Nuclear Propulsion Project Quarterly Progress Report for Period Ending September 10, 1956, USAEC Report ORNL-2157 (Parts 1–5), p. 128.

14. Sax, N., N. Chu, R. H. Miles, and R. W. Miles, Determination of Nitrogen in Lithium, USAEC Report NDA-38 (June, 1957).

15. Leddicotte, G. W., Analytical Chemistry Division Annual Progress Report for Period Ending December 31, 1957, USAEC Report ORNL-2453, p. 30.

16. Still, J. E., "The Determinations of Gases in Metal by Vacuum Fusion," Symposium on the Determination of Gases in Metals, Special Report No. 68, Iron and Steel Institute, London, 1960, pp. 43–63.

17. Gray, R. J., and E. L. Long, Jr., "Polishing by Vibration," Metal Progress, 74(4), 145–48 (1958).

18. Hoffman, E. E., Corrosion of Materials by Lithium at Elevated Temperatures, USAEC Report ORNL-2674 (March, 1959).

19. Lapitskii, A. V., "Anhydrous Lithium Metaniobate," Journal of General Chemistry of the USSR (English Translation), 22, 41–43 (1952).

20. Lapitskii, A. V., and Yu. P. Simanov, "Lithium Salts of Orthoniobic and Orthotantali Acid," Vestnik Moskovskogo Universiteta Seriya Fiziko-Mathematecheskikh i Estestvennykh Nauk No. 1, 9(2), 69–72 (1954).

21. Krylov, E. I., and A. A. Sharnin, "Synthesis and Properties of Niobium Bronzes," Journal of General Chemistry of the USSR (English Translation), 25, 1637–40 (1955).

22. Stephenson, R. L., and H. E. McCoy, Metals and Ceramics Division Annual Progress Report for Period Ending May 31, 1962, USAEC Report ORNL-3313, pp. 42–44.

23. Nowich, A. S., Progress in Metal Physics, 4, 37 (1953).

24. Entwistle, K. M., Metallurgical Reviews, 7(26), 175–239 (1962).

25. Hobson, D. O., Aging Phenomenon in Columbium-Base Alloys, USAEC Report ORNL-3245 (March, 1962), p. 7.

26. DiStefano, op. cit., ORNL-3424, p. 37.

27. Litman, A. P., Determination of Oxygen in Potassium, USAEC Report ORNL-3545 (to be published).

28. Ang, C. Y., "Activation Energies and Diffusion Coefficients of Oxygen and Nitrogen in Niobium and Tantalum," Acta Metallurgica, 1, 124 (1953).

THIS PAGE

WAS INTENTIONALLY

LEFT BLANK

ORNL-3551
UC-25 — Metals, Ceramics, and Materials
TID-4500 (26th ed.)

INTERNAL DISTRIBUTION

1. Biology Library
2-4. Central Research Library
5. Reactor Division Library
6-7. ORNL — Y-12 Technical Library Document Reference Section
8-27. Laboratory Records Department
28. Laboratory Records, ORNL R.C.
29. E. G. Bohlmann
30. G. W. Clark
31. E. L. Compere
32. J. W. Cooke
33. D. R. Cuneo
34. J. E. Cunningham
35. V. A. DeCarlo
36-45. J. R. DiStefano
46. J. H Frye, Jr.
47. R. G. Gilliland
48. R. J. Gray
49. J. C. Griess
50. Karl W. Haff
51. H. L. Hemphill
52-56. M. R. Hill
57. H. Inouye
58. C. E. Larson
59. H. G. MacPherson
60. W. D. Manly
61. F. R. McQuilkin
62. L. R. Phillips
63. R. E. Reed
64. S. A. Reed
65. M. J. Skinner
66. J. A. Swartout
67. W. C. Thurber
68. D. B. Trauger
69. A. M. Weinberg
70. A. A. Burr (consultant)
71. J. R. Johnson (consultant)
72. C. S. Smith (consultant)
73. R. Smoluchowski (consultant)

EXTERNAL DISTRIBUTION

74-75. David F. Cope, AEC, ORO
76. C. M. Adams, Jr., MIT
77. D. E. Baker, GE Hanford
78. T. D. Cooper, ASD, Wright-Patterson AFB
79. Ersel Evans, GE Hanford
80. J. L. Gregg, Cornell University
81. E. E. Hoffman, GE Cincinnati
82. W. A. McNeish, Universal Cyclops
83. T. A. Moss, NASA-SEPO
84. J. Simmons, AEC, Washington
85. E. E. Stansbury, University of Tennessee
86. Donald K. Stevens, AEC, Washington
87. Research and Development Division, AEC, ORO
88-668. Given distribution as shown in TID-4500 (26th ed.) under Metals, Ceramics, and Materials category (75 copies — OTS)